Accepted Manuscript

Identification of Pyrazolo[3,4-e][1,4]thiazepin based CYP51 inhibitors as potential Chagas disease therapeutic alternative: *In vitro* and *in vivo* evaluation, binding mode prediction and SAR exploration

Ludmila Ferreira de Almeida Fiuza, Raiza Brandão Peres, Marianne Rocha Simões-Silva, Patricia Bernardino da Silva, Denise da Gama Jaen Batista, Cristiane França da Silva, Aline Nefertiti Silva da Gama, Tummala Rama Krishna Reddy, Maria de Nazaré Correia Soeiro

Please cite this article as: L.F. de Almeida Fiuza, Raiza.Brandã. Peres, M.R. Simões-Silva, P.B. da Silva, D. da Gama Jaen Batista, Cristiane.Franç. da Silva, A.N.S. da Gama, T.R. Krishna Reddy, M. de Nazaré Correia Soeiro, Identification of Pyrazolo[3,4-e][1,4]thiazepin based CYP51 inhibitors as potential Chagas disease therapeutic alternative: *In vitro* and *in vivo* evaluation, binding mode prediction and SAR exploration, *European Journal of Medicinal Chemistry* (2018), doi: 10.1016/j.ejmech.2018.02.020.

1 **Identification of Pyrazolo[3,4-e][1,4]thiazepin based CYP51 inhibitors as**

2 **potential Chagas disease therapeutic alternative: *In vitro* and *in vivo* evaluation,**

3 **binding mode prediction and SAR exploration**

4

5 Ludmila Ferreira de Almeida Fiuza[1], Raiza Brandão Peres[1], Marianne Rocha Simões-

6 Silva[1], Patricia Bernardino da Silva[1], Denise da Gama Jaen Batista[1], Cristiane França

7 da Silva[1,] Aline Nefertiti Silva da Gama[1], Tummala Rama Krishna Reddy[2] and Maria

8 de Nazaré Correia Soeiro*[1]

9

10 [1] Laboratório de Biologia Celular, Instituto Oswaldo Cruz, Fundação Oswaldo Cruz,

11 Rio de Janeiro, Rio de Janeiro, Brazil.

12 [2] School of Health, Sport and Bioscience, College of Applied Health and

13 Communities, University of East London, Stratford campus, Water Lane, UK.

14

15

16 * Corresponding author at Av. Brasil, 4365 Manguinhos, Rio de Janeiro, Brazil. Phone:

17 55 21 2562-1368; fax: 055 21 2598-4577

18 Email address: soeiro@ioc.fiocruz.br (M.N.C. Soeiro)

19

20 **Running title:** Pyrazolo[3,4-e][1,4]thiazepin activity against *T.cruzi*

21

22

Highlights

- Structure based studies predicted the binding of novel CYP51 inhibitor with CYP51Tc.

- The compounds **1** and **1f** displayed trypanocidal effect upon *T.cruzi in vitro.*

- Compound **1f** gave no effect in vivo, while compound **1** reduced the parasitemia peak.

Graphical abstract
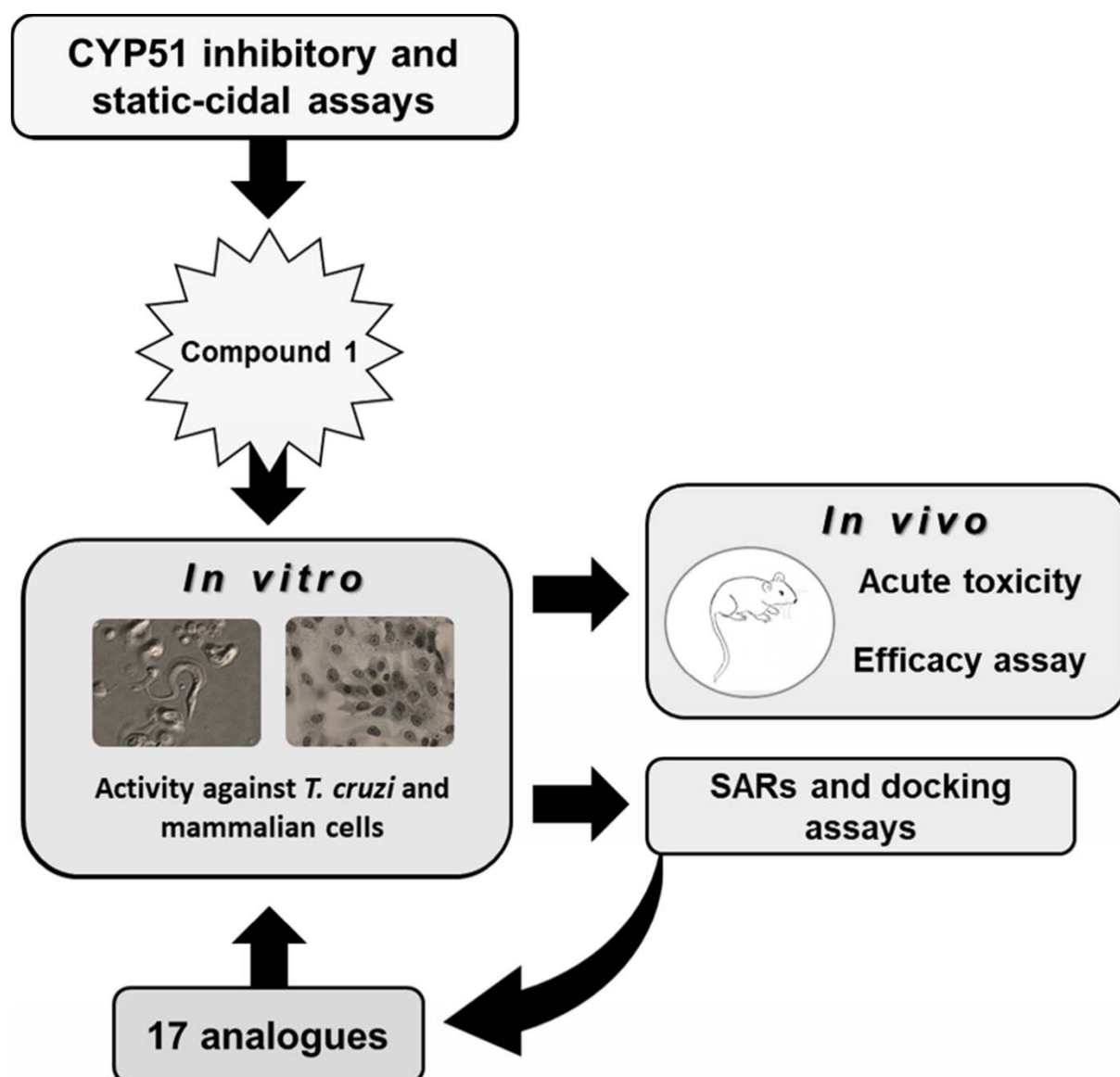
33 **Abstract**

34 American trypanosomiasis or Chagas disease (CD) is a vector borne pathology caused by the

35 parasite *Trypanosoma cruzi (T. cruzi)*, which remains a serious global health problem. The

36 current available treatment for CD is limited to two nitroderivatives with limited efficacy and

37 several side effects. The rational design of ergosterol synthetic route inhibitors (e.g. CYP51

38 inhibitors) represents a promising strategy for fungi and trypanosomatids, exhibiting excellent

39 anti-*T.cruzi* activity in pre-clinical assays. In the present work, we evaluate through different

40 approaches (molecular docking, structure activity relationships, CYP51 inhibitory assay, and

41 phenotypic screenings *in vitro* and *in vivo*) the potency and selectivity of a novel CYP51

42 inhibitor (compound **1**) and its analogues against *T.cruzi* infection. Regarding anti-parasitic

43 effect, compound **1** was active i*n vitro* with EC_{50} 3.86 and 4.00 µM upon intracellular

44 (Tulahuen strain) and bloodstream forms (Y strain), respectively. *In vivo* assays showed that

45 compound **1** reduced in 43 % the parasitemia peak but, unfortunately failed to promote animal

46 survival. In order to promote an enhancement at the potency and pharmacological properties,

47 17 new analogues were purchased and screened *in vitro*. Our findings demonstrated that five

48 compounds were active against intracellular forms, highlighting compounds **1e** and **1f**, with

49 EC_{50} 2.20 and 2.70 µM, respectively, and selectivity indices (SI) = 50 and 36, respectively.

50 Against bloodstream trypomastigotes, compound **1f** reached an EC_{50} value of 20.62 µM, in a

51 similar range to Benznidazole, but with low SI (3). Although improved the solubility of

52 compound **1**, the analogue **1f** did not enhance the potency *in vitro* neither promote better *in*

53 *vivo* efficacy against mouse model of acute *T.cruzi* infection arguing for the synthesis of novel

54 pyrazolo[3,4-e][1,4]thiazepin derivatives aiming to contribute for alternative therapies for CD

55

56

58

1. Introduction

Chagas disease (CD) is a parasitic infection caused by the protozoan *Trypanosoma cruzi* (*T. cruzi*). Considered, as a worldwide public health problem due to migration flows and non-vector transmission routes, is estimates that about 6 to 7 million people are carries of *T.cruzi* and an average of over 12,000 people die every year [1, 2]. The main mechanism of transmission includes: classical vectorial transmission by triatomine bugs also known as blood sucking bugs, via congenital when the parasite is transmitted from mother to child, by oral contamination through ingesting the parasite on contaminated food or drink and through iatrogenic that comprehend blood transfusion or organ transplantation [3]. In many endemic countries like Brazil, vector and blood bank control measures lead to a drastic decreased in the number of new cases via classical vectorial route however, in last decades the oral transmission has emerged with epidemiological relevance in the Amazon region [2]. The CD has two phases, the acute phase appears soon after infection and is characterizing by the patent parasitemia and mostly displaying oligosymptoms ranging from flu-like to intense myocarditis. Due to immune host response, there is a control of the parasite load and most patients move to a later stage called the chronic phase. Although most stay at the indeterminate stage, about 30-40% may develop symptoms after 10 to 20 years post infection mainly related to cardiomyopathy associated or not to gastrointestinal effects [1,4]. The CD available treatment is restricted to two oral nitroheterocyclic compounds, nifurtimox and benznidazole (Bz) both introduced in clinical more than 50 years ago. Even though 25 million people are at risk of infection, according to the WHO, less than 1% of infected patients receive treatment [5]. Thus, the development of new effective drugs for Chagas disease is urgently needed, a

83   neglected pathology that mostly affects poor regions, and with low interest by the

84   pharmaceutical companies due to the low monetary welfares. In addition, other

85   limitations of using the current nitro-derivative drugs are: varying results according to

86   the disease stage, treatment period and dose, age and geographical origin of the

87   patients, side effects, besides a natural resistance profile of some parasite strains

88   against nitro-derivatives [1, 6, 7, 8]. In order to face the limitations of the available

89   therapy, several *in vitro* and *in vivo* studies of potentials new drug candidates for CD

90   have been performed; some of these studies involving inhibitors of the ergosterol

91   biosynthesis pathway. Differently from mammalian cells, in fungi and trypanosomatids,

92   the cytochrome P450 enzyme or sterol 14α-demethylase (CYP51) pathway leads to

93   formation of ergosterol-like products, which are essential for the survival of these

94   parasites, producing viable membranes and making possible cell growth and division

95   [9,10]. Recently, two CYP51 inhibitors first introduced as antifungal, Posaconazole

96   and E1224 (the prodrug of Ravuconazole) and that later showed *in vitro* and *in vivo*

97   efficacy against *T. cruzi* were moved for clinical trials upon chronic Chagas disease

98   patients. Unsuccessfully, both inhibitors demonstrated therapeutic failure as compared

99   to the reference drug, Bz [3, 11]. Among several possibilities, the disappointing results

100   could be related to the lack of translation from *in vitro* and *in vivo* models as compared

101   to the clinic trials as well as lack of pharmacological ideal conditions for human

102   therapy. In fact, the efficacy of the CYP51 inhibitors may be related to the dose and

103   time of exposure. It has been proposed that in clinical trials the administrated dose

104   was inferior to those reached in pre-clinical analysis required to sustain the

105   trypanocidal effect. Also, longer drug therapy administration could have improved their

106   clinical trial efficacy [12, 13, 14]. Then, this class of compounds should be more

107   studied in pre-clinical studies as the parasite is dependent on endogenous sterols and

108 their products, reinforcing the purpose to study CYP51 inhibitors as potential treatment

109 to CD [15, 16, 17]. Also, it must be considering others CYP51 inhibitors molecules, like

110 imidazolic compounds VNI and VFV, that revealed very promising activity against a

111 variety of *T. cruzi* strains *in vitro* and *in vivo* including a high stringent male mouse

112 experimental model [10, 18 19, 20]. These findings reinforces the need to test the

113 potential activity of novel inhibitors of CYP51 more potent and selective and that could

114 be designed with optimized pharmacological properties, besides presenting reduced

115 production cost, and which would allow treatment to be carried out for extended

116 periods of time [10, 16, 20]. Thus, the aim of this study was to evaluate the anti-

117 parasitic activity of a novel pyrazolo[3,4-e][1,4]thiazepin based CYP51 inhibitor

118 (compound **1**) and its 17 analogues through different *in silico, in vitro* and *in vivo*

119 analysis.

120

2. Results and discussion

122 Compound dataset was prepared using commercially available compounds, which

123 cover the broad chemical landscape from the Asinex supplier of ZINC database

124 (release 6). A dataset of 240,000 compounds was extracted (smiles format) based on

125 "lead-like" properties such as Molecular weight between 150 and 500, H-bond donor

126 ≤5, H-bond acceptors ≤ 10, XlogP ≤ 5, Number of rotatable bonds ≤ 8. The minimum

127 cut off for the molecular weight was chosen as 150 to avoid the selection of reagent

128 like molecules. 2D-fingerprints in combination with tanimoto distances were used to

129 select a diverse set of 100 compounds. These compounds were screened for their *in*

130 *vitro* efficacy against intracellular *T.cruzi* amastigotes (strain: Silvio X10/7) in a single

131 replicate at 5 μM. Five compounds that showed >80 % growth inhibition of intracellular

132   amastigotes were selected and a 10-point dose-response curves was carried out to

133   determine their potency. We next assessed these compounds in the static-cidal and

134   CYP51$_{Tc}$ assays. Here, we discuss an interesting compound **1** (MW 413.93; cLogP

135   4.84; H-bond acceptors 4; H-bond donors 2; Number of rotatable bonds 4) with a

136   pyrazolo[3,4-e][1,4] thiazepin scaffold that showed strong CYP51$_{Tc}$ inhibition, with

137   activity comparable to Nifurtimox (Figure 1). This compound demonstrated an EC$_{50}$ of

138   0.4 µM against intracellular Silvio X10/7 parasites, cidal nature (rate of kill assay) with

139   minimum cidal concentration (MCC) of 17 µM (Figure 2) and CYP51$_{Tc}$ inhibition with

140   an IC$_{50}$ of 0.1 µM (Figure 3). Both potency and cidal nature of this compound are

141   compared to Nifurtimox in Table 1.
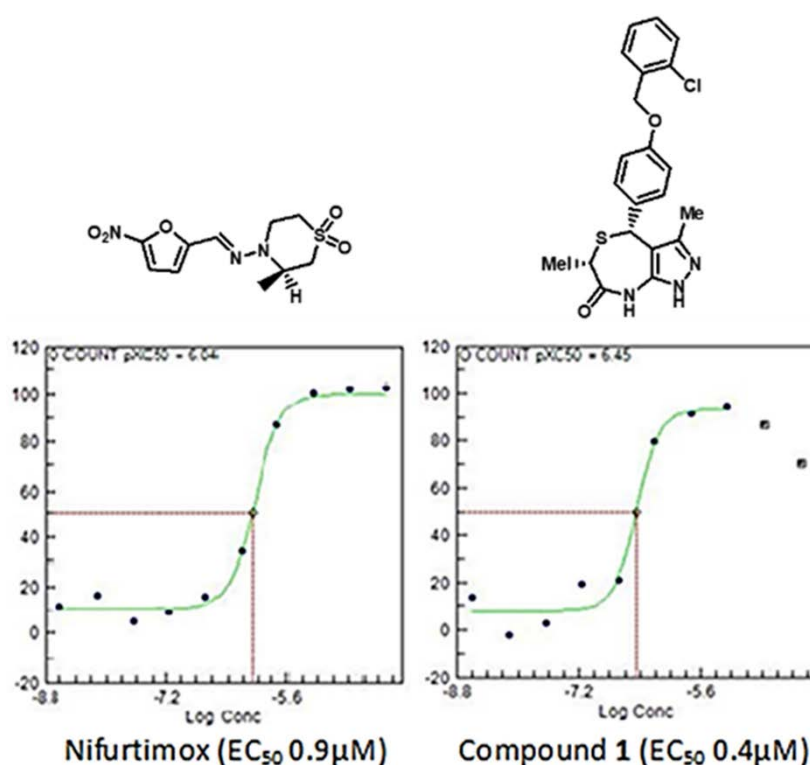
142
143   **Figure 1.** *Molecular structures and ten point dose response curves of Nifurtimox and*
144   *compound **1** with calculated potency values. The X-axis shows log of compound molar*
145   *concentrations (M) and Y-axis shows the normalized activity based on the*
146   *measurement of number of amastigotes per host cell.*
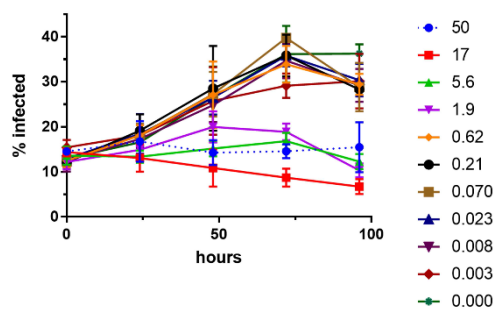
Figure 2. Rate-of-kill assay for compound 1. Ten concentrations of compound were tested. Growth curves are shown for the compound at different concentrations indicated on the right hand side of each growth-line (μM). The level of infection was assessed every 24 hours for 96 hours. Dotted line represents concentration at which host cell toxicity was observed. All measurements are the average of three replicates.

Table 1. Potency assay and Static-cidal (SC) assay results for control compound Nifurtimox and compound 1

Compound	MAX PI * (Static Cidal)	Activity against Silvio X10/7 strain, EC_{50} (μM)
Nifurtimox	103	0.9
Compound 1		

*Maximum Percent Inhibition in the static cidal assay, only derived from compound concentrations that are not toxic to the host cells.

Inhibitory effect of compound 1 on CYP51$_{Tc}$ activity
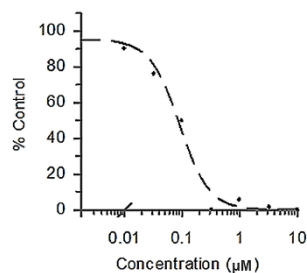
Figure 3. T.cruzi CYP51 Inhibition Assay results for the compound 1 showing an IC$_{50}$ value of 0.1 µM. 'Y' axis range 95.02 (std. error 4.94), slope factor 1.70 (std. error 0.39). Refer supporting information for test concentrations and associated data.

Compound **1** was tested in a fluorescence based functional assay [21] using

recombinant expressed *T.cruzi* CYP51 (Tulahuen strain). Posaconazole was used as

a reference compound. Compound **1** showed potent inhibition of *T.cruzi* CYP51 with

IC$_{50}$ value of 0.1 µM (Figure 3), whereas Posaconazole displayed an IC$_{50}$ value of

0.048 µM (refer supporting information). In a similar assay, Riley et al. [21] reported an

IC$_{50}$ value of 0.880 µM for Fluconazole. Overall compound **1** displayed over 8-fold

more inhibitory activity than Fluconazole and 2-fold less inhibitory activity than

Posaconazole.

As compound **1** showed good potency, cidal nature and strong CYP51$_{Tc}$ inhibition, we

have selected this compound for further development. Initially we have assessed the

178   binding interactions of compound **1** with CYP51 using structure based drug design in

179   order to gain deeper understanding of the interactions at the molecular level. Further,

180   we have tested this compound against other strains of *T.cruzi* representatives of

181   distinct parasite discrete type units - DTUs (Tulahuen – DTU VI and Y, DTU II).

182   **Binding Mode Prediction and Molecular interactions analysis of compound 1**

183   The ligand present in the CYP51$_{Tc}$ (PDB ID: 4C27) crystal structure was re-docked to

184   validate the docking protocol, which was able to successfully reproduce the binding

185   mode observed in the crystal structure. The RMSD value between the heavy atoms of

186   the GLIDE-predicted pose and the crystallographic binding pose is 0.41 A°. We used

187   this docking protocol to dock compound **1** to CYP51$_{Tc}$.
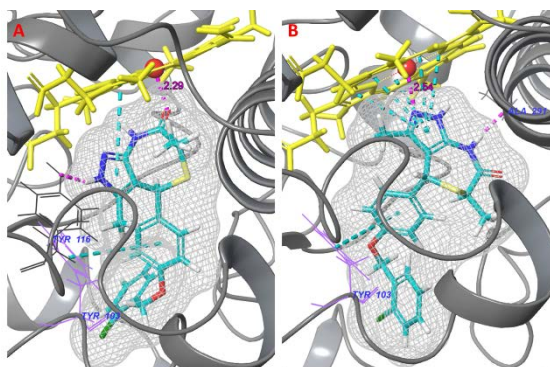
188

189   198
190   199
191   200
192
193
194
195
196
197

Figure 4: Predicted binding poses (A and B) of compound 1 (Teal sticks).

CYP51 of T. cruzi is represented as a transparent surface with cartoon secondary structure. Heme in yellow sticks, Fe in red CPK model. Compound 1 representation: Van der Waals surface around the compound 1 in mesh format, nitrogen in blue, oxygen in red, sulfur in yellow, chlorine in green. Heme iron co-ordination for both binding poses (A and B) in magenta dotted lines. π-π stacking interactions between pyrazole ring and heme macromolecule in teal dashed lines. Side chains of the amino acid residues (wire format) involved in interactions with compound 1 (A, B) through either π-π stacking (Teal dashed lines) or hydrogen bonding (magenta dashed lines). All structure based drug design Images in this article are generated using Schrödinger drug design software.

201   Docking studies predicted two binding poses for compound **1** (Figure 4). In both the

202   poses, the benzyloxy phenyl moiety attached to the basic scaffold pyrazolo-thiazepin

203   mainly occupies the hydrophobic cleft making good van der Waals and hydrophobic

204   interactions with the surrounding amino acids, but the basic scaffold is in different

205   orientation, and the heme iron coordination is different. In the top scoring **pose 1** (XP

206   GScore = - 9.44), the heme iron coordination is predicted with the carbonyl oxygen of

207   the basic scaffold at a distance of 2.29 Å. The Pyrazole ring of the basic scaffold

208   engages in π-π stacking interactions with the heme macrocycle and hydrogen bonds

209   through N-H group with a hydroxyl oxygen of the B'/C loop residue Tyr116. In addition,

210   the phenyl group undergoes a π-π stacking interaction with the phenyl ring of the B'

211   helix residue Tyr103. In the slightly lower scoring **pose 2** (XP GScore = - 8.66), the

212   heme iron coordination is predicted with the nitrogen atom of the pyrazole ring at a

213   distance of 2.54 Å. Similar to pose 1, the Pyrazole ring undergoes π-π stacking

214   interactions with the heme macrocycle and the phenyl group engages in π-π stacking

215   interaction with the phenyl ring of the B' helix residue Tyr103. In addition, the N-H

216   group of the thiazepin ring hydrogen bonded to the carbonyl oxygen of the I-helix

217   residue Ala291. The proposed hydrogen bond formation with Tyr116, π-π stacking

218   interactions with the heme macrocycle and Tyr103 appear to mimic the

219   posaconazole/flucanozole interactions with the $CYP51_{Tc}$. Overall, both the poses are

220   stabilized in the binding pocket with a network of interactions including Fe-

221   coordination, π-π stacking and hydrogen bonding interactions. It appears that these

222   interactions play a dominant role in the binding affinity of compound **1.**

223   **Evaluation of *in vitro* activity of compound 1 against Tulahuen and Y strains**

224 Compound **1** was further evaluated against intracellular forms of *T cruzi* (Tulahuen

225 strain transfected with the β-galactosidase). The anti-parasitic activity of this

226 compound was measured to determine the EC_{50} values after 96 h of compound

227 incubation. The data showed that compound **1** present considerable reduction in the

228 number of parasite population, with an EC_{50} of 3.86 μM, which is comparable to the

229 activity of reference compound (Bz) that reached an EC_{50} of ∼2.63 μM (Table 2). Our

230 data confirmed that this CYP51 inhibitor is able to act upon different parasite strains

231 (Sylvio-X10/7 and Tulahuen), belonging also to different *T.cruzi* DTUs (I and VI,

232 respectively), which is a very promising characteristic for a novel drug for CD [8].

233 **Table 2.** *Activity (EC_{50} - Mean ± SD) against intracellular forms (Tulahuen B-Galactosidase*
234 *transfected strain) and bloodstream trypomastigotes of T.cruzi (2 and 24h - Y strain).*

Compound	Activity against intracellular forms (EC_{50} μM)	Activity against bloodstream trypomastigotes (EC_{50} μM)	
		2 h	24 h
Benznidazole	2.63 ± 0.49	>10	6.02 ± 1.47
Compound 1	3.86 ± 0.26	>10	4.00 ± 0.35

235

236 Next, as compound **1** displayed a potential activity *in vitro* against intracellular forms of

237 *T. cruzi* (Tulahuen and Sylvio X10/7 strains)*,* this compound was assayed against

238 other relevant forms for mammalian infection, the bloodstream trypomastigotes, using

239 also another parasite strain and DTU (Y strain, DTU II), under a time drug exposure

240 incubation (2 and 24 h). The findings demonstrated that although both compound **1**

241   and Bz were not active after 2 h of incubation (EC_{50} of >10 µM), the CYP51 inhibitor

242   showed trypanocidal effect after longer periods of incubation of BT, with an EC_{50} of ~4

243   µM, and as found for intracellular parasites (Tulahuen strain), with comparable

244   potency as Bz (Table 2) and Nifurtimox (Table 1). We have therefore evaluated a set

245   of selected analogues (**1a**-**1q**, Table 3) with various functional groups that differ in

246 electronic properties, position and steric properties as follows. The phenotypic effect of

247 these compounds was first screened regarding their ability to reduce the infection

248 levels against intracellular forms of *T. cruzi* (Tulahuen strain). Compounds with > 50 %

249 reduction on infection levels using a single concentration (10-12 μM, corresponding

250 the EC_{90} value of Bz, Table 3) were further subjected to potency assays (activity

251 expressed as EC_{50} in Table 3). Toxicity profiles were determined against L929 cell

252 cultures by incubating for 96 h with different concentrations of these compounds and

253 then cell viability evaluated by both light microscopy and colorimetric assay

254 (AlamarBlue tests) and expressing the respective LC_{50} values (Table 3). The ratio of

255 LC_{50} and EC_{50} values is presented in the same table as Selectivity Index (SI),

256 indicating the quantity of compound that is active against the *T.cruzi* but is not toxic

257 264

258 265

259

260

261

262

263

towards the host cell.

266

267

268

Table 3. *Activity (percentage reduction of the L929 culture infection) using a fixed*

concentration (10-12 μM), and anti-parasitic potency (EC$_{50}$ - Mean ± SD – 96 h), mammalian

host cell toxicity (L929 – 96 h) and selectivity against intracellular forms of T.cruzi (Tulahuen

B-Galactosidase transfected strain).

Benznidazole (BZ)   Type 1   Type II

273
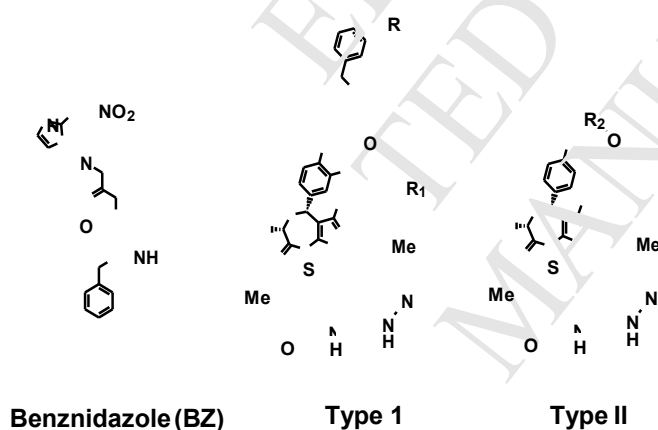
ID	Type	R			R$_1$	R$_2$	% redu... infecti... (si... conce...
		Ortho	*Meta*	*Para*			
Bz	-	-	-	-	-	-	89.3
1	I	Cl	H	H	H	-	
1a	I	H	H	Cl	H	-	14.88
1b	I	F	H	H	H	-	63.64
1c	I	H	F	H	H	-	70.68
1d	I	H	H	F	H	-	32.42
1e	I	Me	H	H	H	-	69.14
1f	I	H	Me	H	H	-	89.2

274   275

266

* EC_{50} data taken from Table 2; i-Pr: isopropyl; n-Pr: n-propyl; nd: not determined

276

277 The *in vitro* analysis revealed that five compounds (**1b**, **1c**, **1e**, **1f** and **1k,** Table 3)

278 were able to decrease the intracellular parasite load in the infected L929 cell cultures,

279 ranging 53 up to 89 % of reduction when concentration equivalent of EC_{90} of Bz was

280 used (Table 3). These compounds also displayed low toxicity profile against

281 mammalian host cells ($LC_{50} \geq 50$ μM**,** table 3). Compounds **1c**, **1e and 1f** did not

282 induce loss of cellular viability after incubation for 96 h with doses up to 98 μM.

283 Compound **1b** maintained mammalian cell viability up to 200 μM. However, compound

284 **1k** exhibited moderate toxicity with LC_{50} of ~50 μM. Compound **1e** displayed high SI

285 value (> 50), comparable to benznidazole. Compounds **1b**, **1c**, **1f** displayed

286 considerable selectivity with SI values >38, >19 and >36 respectively. Although

287 compound **1k** showed moderate potency against intracellular parasites, it showed

288 poor selectivity (SI value = 4.7). An interesting observation from the above results

289 (Table 3) is that compounds with *ortho*-substitutions displayed better selectivity and

290 toxicity profiles when compared with *meta*-substituted compounds (compare SI and

291 LC_{50} values of **1b** with **1c** and **1e** with **1f**) when assayed against intracellular forms of

292 *T. cruzi* (Tulahuen strain). Compounds (**1b**, **1c**, **1e**, **1f** and **1k,** Table 3) showed good

293 *in vitro* potency against intracellular forms of *T. cruzi* (Tulahuen β-Galactosidase

294 transfected strain) were further tested for their activity against bloodstream

276
295   trypomastigotes (Y strain). The results are shown in Table 4. After 2 h of incubation, all

296   compounds showed an EC_{50} of >50 µM, similarly as benznidazole. After 24 h of

297   incubation, compounds **1b**, **1e** and **1k** did not show much improvement in the potency.

298   Compound **1c** showed large variations in potency possibly due to compound

299   instability. Interestingly, compound **1f** showed (EC_{50} of ~20 µM) comparable activity to

300   reference compound (EC_{50} of ~16 µM). The predicted binding pose of compound **1f** is

301 shown in Figure 5 (A). The orientation of the binding pose and the receptor

302 interactions are similar to compound **1**. We have further evaluated all five compounds

303 for their toxicity on primary cell cultures. Uninfected cardiac cells were incubated for 24

304 h with different doses of these compounds and then cell viability evaluated by both

305 light microscopy and colorimetric assay Prestoblue.

306 **Table 4.** *Activity (EC$_{50}$ μM - Mean ± SD – 2 and 24h) against bloodstream trypomastigotes of*
307 *T. cruzi (Y strain) besides toxicity upon cardiac cells (24h) and selectivity profile.*

Compound	EC$_{50}$ μM		LC$_{50}$ μM	SI (LC$_{50}$/EC$_{50}$ – 24 h) μM
	2 h	24 h		
Benznidazole	>50	16.86 ± 3.34	>200	>12
1b	>50	>50	>200	>4
1c	>50	46.98 ± 10.93	93.97 ± 11.73	3.71
1e	>50	38.6 ± 6	>200	>5.2
1f	>50	20.62 ± 6.12	66 ± 25.82	3.20
1k	>50	39.37 ± 6.37	ND*	ND*

308 * ND: Not determined

309 Compounds **1b**, **1e** did not induce loss of cellular viability after incubation for 24 h up

310 to 200 μM (Table 4). Compounds **1c** and **1f** displayed low toxicity with LC$_{50}$ values of

311 ∼93 and ∼66 μM, respectively.

312 **Structure Activity Relationship (SAR) Analysis**

313 Next, the structure activity relationships of these compounds (**1a**-**1q**) is discussed

314 according to their effect towards the infection level and the EC$_{50}$ values against the

315 intracellular parasites. Compounds **1a**-**1g** (Table 3) that differ in the substitution

316   pattern on the benzyl ring showed varied levels of potency. Compound **1** with *ortho-*

317   chloro substitution displayed potency with an EC_{50} of ~3.86 µM. The switching of

318   electron withdrawing, bulky chlorine from *ortho-* position (**1**) to *para-* position (**1a**)

319   resulted in loss of potency. Replacement of *ortho-* chloro substituent with fluoro group

320   (**1b**) displayed potency with an EC_{50} of ~5.30 µM, and the switching of fluoro group

321   from *ortho-* (**1b**) to *meta-* position (**1c**) displayed similar potency. However, *para-*

322   fluoro substituted compound (**1d**) showed poor potency. Replacement of bulky,

323   electron withdrawing *ortho-* chloro group (**1**) with isosteric, isolipophilic and electron

324   donating methyl group (**1e**) displayed improved potency with an EC_{50} of ~2.20 μM, and

325   the switching of methyl group from *ortho-* (**1e**) to *meta-* position (**1f**) retained the

326   potency with an EC_{50} of ~2.70 μM. However, *para-* methyl substitution (**1g**) resulted in

327   complete loss of potency, suggesting that the substitution pattern on the aromatic ring

328   is important.   The general trend of activity being *ortho-* and *meta-* substituted

329   compounds are more potent than *para-* substituted compounds (compare **1** with **1a**;

330   compare **1b**, **1c** with **1d**; compare **1e**, **1f** with **1g**). Overall, *para-* substitutions

331   (chloro/fluoro/methyl; **1a**, **1d**, **1g**) on the benzyl ring generally displayed poor or no

332   potency.   Docking studies on these compounds suggest that *para-* substitutions

333   protrude from the hydrophobic cleft towards a more solvent exposed area, while the

334   *ortho-* and *meta-* substitutions allow better interactions with the hydrophobic cleft. This

335   may explain why all substitutions at the *para-* position (**1a**, **1d**, **1g)** are not tolerated.

336   The results suggest that the electronic properties of the substituents (chlorine moiety

337   being electron withdrawing and methyl moiety being electron donating) did not

338   influence the activity; however, the position specific and hydrophobic effects of the

339   substituents on the benzyl ring are mainly involved in the variation in potency. We next

340   turned our attention to compounds **1h**-**1n** with *ortho*- methoxy substituted phenyl ring.

341   Compound **1h** with unsubstituted benzyloxy group showed poor potency. Compounds

342   with *ortho*- (**1i**, **1l**), *meta*- (**1j**, **1m**) and *para*- substitutions (**1n**) on the benzyl ring also

343   displayed poor or no potency, the only exception is *para*-chloro substitution which

344   resulted in a comparatively potent compound **1k**. Our binding mode analysis of

345   compounds **1i**, **1j**, **1l** and **1m** suggested that the introduction of a bulky methoxy group

346 at the *ortho-* position restricts the conformation of the phenyl ring, thereby resulting in

347 a different orientation, losing key interactions such as coordination with the heme iron,

348 π-π stacking with Tyr103 and hydrogen bonding with Tyr116. This appears to have

349 resulted in loss of potency for these compounds. Interestingly, in the top scored

350 binding poses of compounds **1h**, **1k** and **1n** reverse binding modes were observed,

351 where the pyrazolo [3,4-e] [1,4] thiazepin-7-one scaffold is placed in the hydrophobic

352 binding cleft, benzyloxy moiety is placed in the B'/C loop and I helix region. This

353 reverse binding mode do not appear to have favoured the potency of compounds **1h**

354 and **1n**. However, for compound **1k**, methoxy phenyl ring is in a different orientation

355 compared to **1h** and **1n,** making strong hydrophobic interactions with the surrounding

356 amino acids, thereby displaying moderate   potency with an EC_{50} of ~10.85 µM. The

357 364
     365
     366
     367
     368
     369
     370

358

359
360
361
362
363

binding pose of compound **1k** is shown in Figure 5 (B).

Figure 5: *A) Predicted binding pose of compound **1f** (green sticks; XP GScore -8.58) in the hydrophobic tunnel. Heme iron co-ordination is represented as magenta dotted lines (2.30 Å). π-π stacking interactions between pyrazole ring and heme macromolecule in teal dashed lines. Side chains of the amino acid residues TYR103 (wire format in black) TYR116 (wire format in magenta) involved in interactions with compound **1f** through π-π stacking (teal dashed lines) and hydrogen bonding (magenta dashed lines) respectively. All the interactions of this compound are similar to compound **1** (pose 1). B) Predicted reverse binding pose of **1k** (orange sticks; XP GScore -10.64), pyrazolo [3,4-e] [1,4] thiazepin-7-one ring system is at the entrance of the tunnel and p-chlorophenyl moiety is oriented towards the heme; Heme in yellow sticks, Fe in red CPK model, Van der Waals surface around the compound **1k** in mesh format, nitrogen in blue, oxygen in red, sulfur in yellow. Side chain carbonyl oxygen of the amino acid residue MET358 (wire format in magenta) is involved in*

371 *hydrogen bonding (magenta dashed lines) interaction with the NH moiety (pyrazole ring) of*
372 *compound 1k.*

373 We finally probed the contribution of the substituted benzyl group of the pyrazolo [3,4-

374 e] [1,4] thiazepin-7-one ring system towards the potency by screening a small set of

375 analogues with aliphatic substitutions (Type II). Replacement of benzyl ring with

376 isopropyl (**1o**), n-propyl (**1p**) and allyl (**1q**) moieties completely abolished the potency

377 altogether, suggesting that substituted benzyl ring plays an important role in stabilising

378 the complex by forming strong hydrophobic interactions with the hydrophobic cleft.

379 Moreover, perhaps these aliphatic substitutions do not fill the hydrophobic pocket

380 enough, which was needed for potency and stability. Overall, these results suggest

381 that the coordination with the heme iron, π-π stacking and hydrogen bond interactions

382 in the B'helix and B'/C loop region, and the hydrophobic interactions with the residues

383 surrounding the hydrophobic tunnel are crucial for the potency of this series of

384 compounds.

385 Overall, **1e** and **1f** were the more promising compounds regarding potency and

386 selectivity profiles in both the intracellular (Tulahuen) and bloodstream trypomastigote

387 (Y strain) forms of *T. cruzi* when compared to **1b**, **1c**, and **1k**. Hence, as **1e** showed

388 poor solubility profile, we have further evaluated compounds **1** and **1f** for their *in vivo*

389 activity in mouse models of acute *T.cruzi* infection.

390 **Evaluation of compounds *in vivo***

391 The *in vivo* efficacy of the compound **1** was evaluated using non-toxic doses

392 (previously determined in acute mice toxicity tests, showing an NOAEL > 50 mg/kg -

393 i.p., data not shown) using 5, 10 and 20 mg/kg/daily doses. Bz was tested in parallel at

394 its optimal dose of 100 mg/kg [22]. The administration of compound **1** for five days

395   resulted in a mild reduction in the parasitemia peak levels, being much lower than Bz

396   which reached 100 % of peak suppression. The CYP51 inhibitor reached 30, 38 and

397   43% of reduction in respective doses of 5, 10 and 20 mg/kg/day at the peak of

398   parasitemia, (*Figure 6*). Regarding the mortality, while Bz guaranteed 100 % animal

399   survival, all treated animals with compound **1,** died (*Figure 7*). Unfortunately, using the

400   same mouse experimental model of *T.cruzi* infection, the administration for five

401   consecutive days of 5-20 mg/kg of compound **1f** (non-toxic doses based on previous

402   acute toxicity assays using female Swiss mice) did not induce parasitemia decrease

403   neither protect against animal mortality. Bz was able to completely suppress

404   parasitemia peak (8 dpi) and gave 100 % mice survival (data not shown).

405
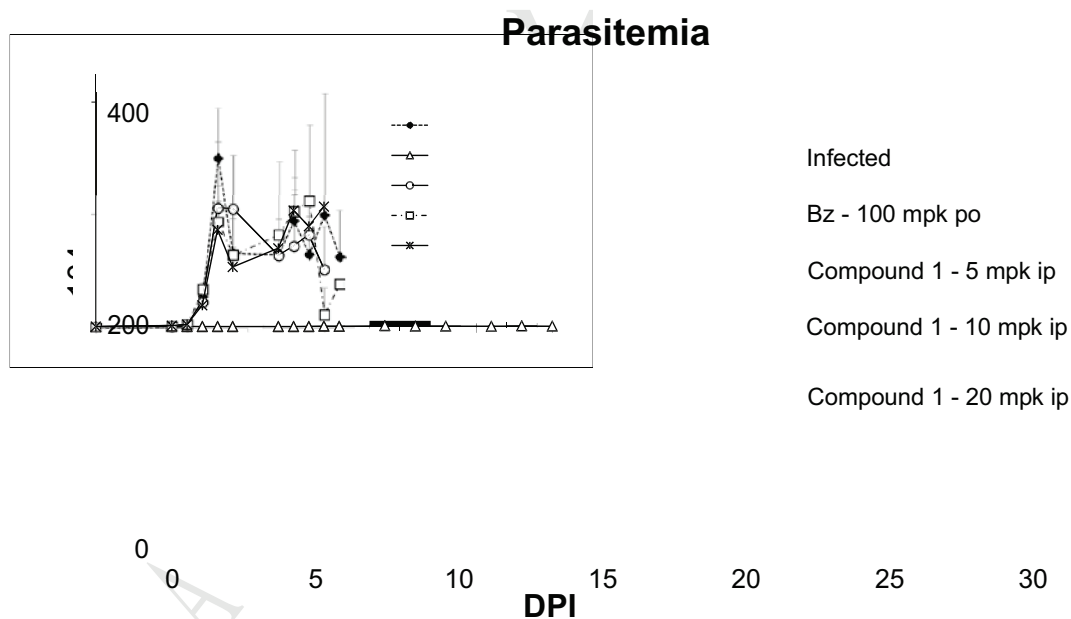
Figure 6. *In vivo effect of Compound **1** (5-20 mg/kg) and Bz (100 mg/kg) upon T.cruzi parasitemia levels using an mouse model of acute infection (Y strain).mpk = mg/kg; DPI: Days post-infection.*
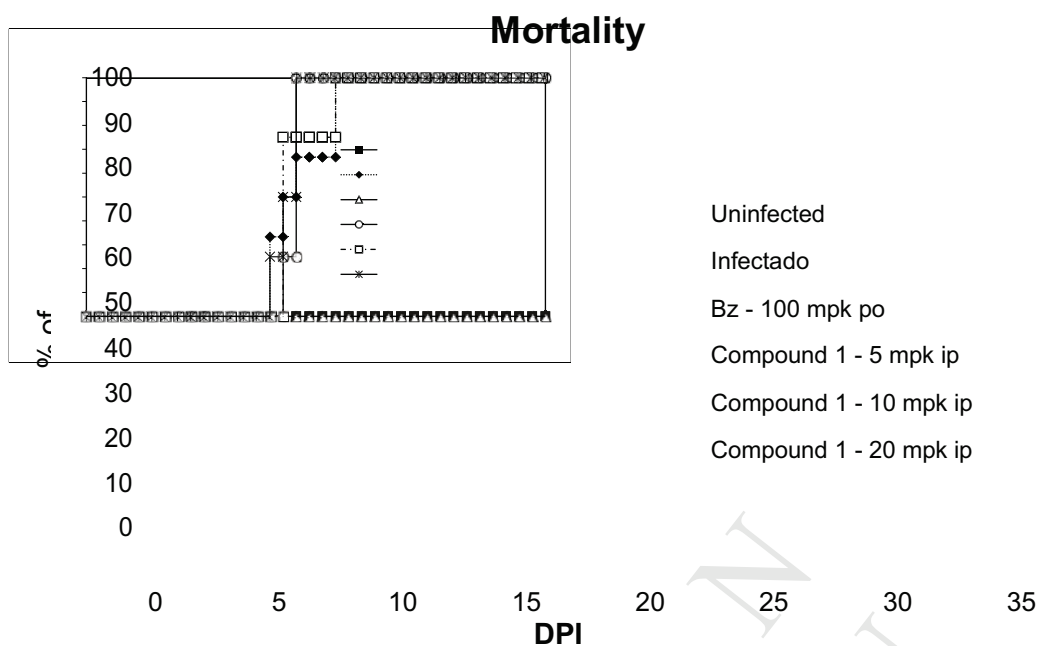
Figure 7. *In vivo effect of Compound 1 (5-20 mg/kg) and Bz (100 mg/kg) upon animal mortality induced by T.cruzi infection using an mouse model of acute infection (Y strain). mpk = mg/kg; DPI:* Days post-infection.

3. Conclusion

Only two drugs are available for the treatment of Chagas disease, and both have

limited efficacy in addition to several adverse effects. So the search for more effective

therapeutic alternatives is urgently needed, to face these limitations CYP51 inhibitors

were suggested due to its specific and selective mechanism of action. In this study we

have focused on the initial lead optimization of pyrazolo[3,4-e][1,4]thiazepin based

lead compound **1**. This compound displayed comparable activity with nifurtimox and

benznidazole, being potent against multiple strains (Sylvio-X10/7, Tulahuen and Y

strain) and forms of *T. cruzi*. Fluorescence based functional assay confirmed that the

425 mode of action of lead compound **1** is via inhibition of $CYP51_{Tc}$. Structure based drug

426 design studies predicted the binding interactions of lead compound **1** with $CYP51_{Tc}$ to

427 be similar to Posaconazole and Fluconazole. A small library of analogues of

428   compound **1** were evaluated for their potency and selectivity profiles against both the

429   intracellular (Tulahuen) and bloodstream trypomastigote (Y strain) forms of *T. cruzi.*

430   This resulted in interesting SARs that are in good agreement with our predicted

431   binding modes. Compound **1f** showed most promising anti-*T.cruzi* activity. Lead

432   compound **1** and compound **1f** were further evaluated for their *in vivo* activity in mouse

433   models of acute *T.cruzi* infection. Compound **1** is only partially effective in the

434   reduction of parasitemia possibly due to limited permeability and solubility

435   characteristics. Compound **1f** failed to reduce the parasitemia possibly due to poor

436   permeability. Solubility and permeability are important physicochemical characteristics

437   of drug like compounds that reflect their bioavailability. The $CYP51_{Tc}$ inhibitors

438   described here provide an excellent template for further lead optimization of

439   pyrazolo[3,4-e][1,4]thiazepin based analogues with improved solubility and

440   permeability properties that may facilitate the anti-*T.cruzi* drug development.

452 **4. Experiment**

453 **Compound database preparation:** All the compounds in the dataset were processed

454 through concord for the three-dimensional structure generation (mol2 files).

455 Compounds with inappropriate isomeric specifications, compounds containing

456 disallowed atoms in terms of valency and compounds with errors in ring definition are

457 excluded from the co-ordinate generation. These compounds were converted into SLN

458 format (SYBYL Line Notation) using UNITY translate module in SYBYL Version 7.3

459 (Tripos) [23]. The selector module was used to generate two dimensional fingerprints

460 and tanimoto distances. All the compounds in this study were purchased from

461 ASINEX.

462 **Molecular docking:** Molecular modelling studies were performed primarily using

463 Schrödinger drug design software suite (Schrödinger Release 2017-2) [24].

464 **Protein preparation:** The $CYP51_{Tc}$ (PDB: 4C27 with a resolution of 1.95 A°) protein

465 structure was retrieved from Protein Data Bank. The protein was initially prepared

466 using the Protein Preparation Wizard module of Schrödinger suite that prepares the

467 protein by adding hydrogens, assigning correct bond orders, creating zero bond

468 orders to metals, fixing errors like missing side chains and adjusting the ionisation and

469 tautomeric states (via Epik). We have deleted all the water molecules, chloride ions

470   and solvents (ethylene glycol) from the protein. Optimisation of the hydrogen bonding

471   network and the orientation of the hydroxyl/thiol groups, terminal amide groups in Asn

472   and Gln, and His states was carried out using the ProtAssign algorithm. Finally,

473   restrained minimization was carried out using all atoms OPLS3 force fields, with

474   converge heavy atoms to RMSD set to 0.3 Ă (default).

475 **Ligand Preparation:** All the compounds were prepared using Ligprep module, which

476 performed addition of hydrogens, 2D to 3D conversion, generation of ionization and

477 tautomeric states including metal binding states (via Epik) at physiological pH 7.0 ±

478 2.0, and also generated possible stereoisomers and ring conformations using default

479 settings. All the compounds were energy minimised using OPLS3 force fields.

480 **Docking studies:** The Receptor Grid generation was carried out by identifying the

481 ligand in the 4C27 crystal structure and excluding it from the grid generation. The grid

482 covers the entire binding site, which includes the heme iron macromolecule. Metal

483 coordination constraint was applied at the Fe atom of the heme that defines an

484 interaction between the ligand atom and the heme iron. Docking of compounds was

485 carried out using Schrödinger GLIDE, in extra precision (XP) mode.

486 **CYP51 inhibitory assay:** The CYP51 assay was carried out as described in [21]. All

487 the potency assays and rate of kill assays with *T. cruzi* Silvio X10/7 strain were carried

488 out as described in [25].

489 **Spectroscopic data analysis and compound purity assessment by HPLC**

490 All 18 compounds were purchased directly from Asinex and used as supplied unless

491 otherwise stated. Accurate mass and nominal mass measurements were performed

492 using Bruker micrOTOF mass spectrometer. All ^{1}HNMR spectra were recorded in

493   deutero-DMSO in 5 mm tubes, with tetramethylsilane as an internal standard, using a

494   Bruker instrument. Chemical shifts (δ) are reported in ppm, and coupling constants (J)

495   are given in Hz. Signals are represented by s (singlet), d (doublet), t (triplet), q

496   (quartet), dq (double quartet) m (multiplet), bs (broad singlet), and dd (double doublet).

497   HPLC was carried out using Agilent-1200 instrument. Column: Agilent eclipse plus

498   C18 (150mm $\times$ 4.6mm, 5µm particle size), mobile phase 0.01% TFA in

499   acetonitrile/water (5% to 95% organic over 20min at 1mL/min), 10 μL injection.

500   Detection was at 254nm, runtime 25 min. All the samples were prepared by dissolving

501   the 5mg of compound in 0.7 mL of d^6-DMSO (Sample solution prepared for HNMR

502   was analyzed by HPLC). Blank (without the compound) d^6-DMSO was used as a

503   reference standard. Most of the compounds displayed >90% purity except compounds

504   **1h** (77%), **1j** (88%), **1l** (87%) and **1n** (84%). Refer to the supporting information for

505   complete data on HPLC purity analysis. Isomer ratios of the compounds were

506   calculated from ^{1}H-NMR spectra based on the CH_3 signal (s) from substituted pyrazole

507   ring of the one of the isomer against CH_3 signal (s) from substituted pyrazole ring of

508   the other isomer.

509   *4-[4-(2-Chloro-benzyloxy)-phenyl]-3,6-dimethyl-4,8-dihydro-1H-pyrazolo[3,4-*

510   *e][1,4]thiazepin-7-one* (**Compound 1**). Mixture of two isomers (98:2), δ_H/ppm (400

511   MHz, d^6-DMSO): Major isomer peaks are at 12.32 (1H, bs, NH from 3-pyrazole ring),

512   9.66 (1H, s, NH from sec.amide), 7.62-7.55 (1H, m, Ar-H), 7.54-7.46 (1H, m, Ar-H),

513   7.43-7.34 (2H, m, Ar-H), 7.21 (2H, d, J = 8.7 Hz, Ar-H), 6.94 (2H, d, J = 8.7 Hz, Ar-H),

514   5.56 (1H, s, methine from [1,4] thiazepin ring), 5.11 (2H, s, CH_2), 3.68 (1H, q, J = 7.0,

515   methine from [1, 4] thiazepin ring), 1.91 (3H, s, CH_3 from pyrazole ring), 1.19 (3H, d, J

516   = 7.0 Hz, CH_3 from [1, 4] thiazepin ring); Observable minor isomer peaks are at 9.86

517   (1H, s, NH from sec.amide), 7.0 (2H, d, J = 8.8 Hz, Ar-H), 5.33 (1H, s, methine from

518   [1, 4] thiazepin ring), 5.14 (2H, s, CH_2), 1.69 (3H, s, CH_3 from pyrazole ring), 1.08 (3H,

519   d, J = 7.1 Hz, CH_3 from [1, 4] thiazepin ring). HRMS-m/z (ESI): found 414.1046

520   ($C_{21}H_{22}N_3O_2S$ $[M + H]^+$) requires 414.0965.

521   *4-[4-(4-Chloro-benzyloxy)-phenyl]-3,6-dimethyl-4,8-dihydro-1H-pyrazolo[3,4-*

522   *e][1,4]thiazepin-7-one* **(1a)**. Mixture of two isomers (96:4), δ_H/ppm (400 MHz, d^6-

523 DMSO): Major isomer peaks are at 12.31 (1H, s, NH from 3-pyrazole ring), 9.65 (1H,

524 s, NH from sec.amide), 7.48-7.41 (4H, m, Ar-H), 7.19 (2H, d, J = 8.7 Hz, Ar-H), 6.91

525 (2H, d, J = 8.7 Hz, Ar-H), 5.55 (1H, s, methine from [1, 4] thiazepin ring), 5.05 (2H, s,

526 CH$_2$), 3.67 (1H, q, J = 7.04 Hz, methine from [1, 4] thiazepin ring), 1.90 (3H, s, CH$_3$

527 from pyrazole ring), 1.18 (3H, d, J = 7.08 Hz, CH$_3$ from [1,4] thiazepin ring);

528 Observable minor isomer peaks are at 9.86 (1H, s, NH from sec.amide), 6.97 (2H, d, J

529 = 8.7 Hz, Ar-H), 5.32 (1H, s, methine from [1, 4] thiazepin ring), 5.08 (2H, s, CH$_2$), 1.68

530 (3H, s, CH$_3$ from pyrazole ring), 1.07 (3H, d, J = 7.2 Hz, CH$_3$ from [1, 4] thiazepin ring).

531 HRMS-m/z (ESI): found 414.1042 (C$_{21}$H$_{22}$N$_3$O$_2$S [M + H]$^+$), requires 414.0965.

532 *4-[4-(2-Fluoro-benzyloxy)-phenyl]-3,6-dimethyl-4,8-dihydro-1H-pyrazolo[3,4-*

533 *e][1,4]thiazepin-7-one* **(1b).** Mixture of two isomers (95:5), δ$_H$/ppm (400 MHz, d^6-

534 DMSO): Major isomer peaks are at 12.31 (1H, bs, NH from 3-pyrazole ring), 9.66 (1H,

535 s, NH from sec.amide), 7.58-7.50 (1H, m, Ar-H), 7.46-7.37 (1H, m, Ar-H), 7.29-7.15

536 (2H, m, Ar-H) this multiplet is overlapped with doublet from the aromatic ring that is

537 directly attached to the pyrazolo[3, 4-e][1, 4]thiazepin basic scaffold, 7.20 (2H, d, J =

538 8.7 Hz, Ar-H), 6.94 (2H, d, J = 8.7 Hz, Ar-H), 5.56 (1H, s, methine from [1, 4] thiazepin

539 ring), 5.09 (2H, s, CH$_2$), 3.68 (1H, q, J = 7.0 Hz, methine from [1, 4] thiazepin ring),

540 1.91 (3H, s, CH$_3$ from pyrazole ring), 1.19 (3H, d, J = 7.0 Hz, CH$_3$ from [1,4] thiazepin

541 ring); Observable minor isomer peaks are at 9.85 (1H, s, NH from sec.amide), 6.94

542 (2H, d, J = 8.7 Hz, Ar-H), 5.56 (1H, s, methine from [1, 4] thiazepin ring), 5.11 (2H, s,

543 CH_2), 1.68 (3H, s, CH_3 from pyrazole ring), 1.07 (3H, d, J = 7.2 Hz, CH_3 from [1, 4]

544 thiazepin ring). ^{19}FNMR: 118.41 ppm. HRMS-m/z (ESI): found 398.1341

545 ($C_{21}H_{21}FN_3O_2S$ [M + H]$^+$), requires 398.1260.

546 *4-[4-(3-Fluoro-benzyloxy)-phenyl]-3,6-dimethyl-4,8-dihydro-1H-pyrazolo[3,4-*

547 *e][1,4]thiazepin-7-one* **(1c).** Mixture of two isomers (86:14), δH/ppm (400 MHz, d^6-

548 DMSO): Major isomer peaks are at 12.30 (1H, bs, NH from 3-pyrazole ring), 9.65 (1H,

549 s, NH from sec.amide), 7.47-7.38 (1H, m, Ar-H), 7.31-7.23 (2H, m, Ar-H), 7.16-7.12

550 (1H, m, Ar-H) this multiplet is overlapped with doublet from the aromatic ring that is

551 directly attached to the pyrazolo[3, 4-e][1, 4]thiazepin basic scaffold, 7.19 (2H, d, J =

552 8.7 Hz, Ar-H), 6.92 (2H, d, J = 8.7 Hz, Ar-H), 5.55 (1H, s, methine from [1, 4] thiazepin

553 ring), 5.08 (2H, s, CH$_2$), 3.67 (1H, q, J = 7.03 Hz, methine from [1, 4] thiazepin ring),

554 1.90 (3H, s, CH$_3$ from pyrazole ring), 1.19 (3H, d, J = 7.08 Hz, CH$_3$ from [1,4] thiazepin

555 ring); Observable minor isomer peaks are at 9.85 (1H, s, NH from sec.amide), 6.97

556 (2H, d, J = 8.7 Hz, Ar-H), 5.32 (1H, s, methine from [1, 4] thiazepin ring), 5.10 (2H, s,

557 CH$_2$), 3.24 (1H, q, J = 1.67 Hz),1.67 (3H, s, CH$_3$ from pyrazole ring), 1.06 (3H, d, J =

558 7.2 Hz, CH$_3$ from [1, 4] thiazepin ring). ^{19}FNMR: 113.20 ppm. HRMS-m/z (ESI): found

559 398.1341 (C$_{21}$H$_{21}$FN$_3$O$_2$S [M + H]$^+$), requires 398.1260.

560 *4-[4-(4-Fluoro-benzyloxy)-phenyl]-3,6-dimethyl-4,8-dihydro-1H-pyrazolo[3,4-*

561 *e][1,4]thiazepin-7-one (1d)*. Mixture of two isomers (96:4), δH/ppm (400 MHz, d^6-

562 DMSO): Major isomer peaks are at 12.33 (1H, bs, NH from 3-pyrazole ring), 9.65 (1H,

563 s, NH from sec.amide), 7.54-7.44 (2H, m, Ar-H), 7.25-7.16 (4H, m, Ar-H), 6.91 (2H, d,

564 J = 8.7 Hz, Ar-H), 5.55 (1H, s, methine from [1, 4] thiazepin ring), 5.03 (2H, s, CH$_2$),

565 3.67 (1H, q, J = 7.02 Hz, methine from [1, 4] thiazepin ring), 1.90 (3H, s, CH$_3$ from

566 pyrazole ring), 1.19 (3H, d, J = 7.08 Hz, CH_3 from [1,4] thiazepin ring); Observable

567 minor isomer peaks are at 9.85 (1H, s, NH from sec.amide), 6.96 (2H, d, J = 8.7 Hz,

568 Ar-H), 5.32 (1H, s, methine from [1, 4] thiazepin ring), 5.05 (2H, s, CH_2), 1.67 (3H, s,

569 CH_3 from pyrazole ring), 1.07 (3H, d, J = 7.1 Hz, CH_3 from [1, 4] thiazepin ring).

570 ^{19}FNMR: 114.49 ppm. HRMS- m/z (ESI): found 398.1340 ($C_{21}H_{21}FN_3O_2S$ [M + H]$^+$),

571 requires 398.1260.

572 *3,6-Dimethyl-4-[4-(2-methyl-benzyloxy)-phenyl]-4,8-dihydro-1H-pyrazolo[3,4-*

573 *e][1,4]thiazepin-7-one* (**1e**). Mixture of two isomers (97:3), δH/ppm (400 MHz, d^6-

574 DMSO): Major isomer peaks are at 12.30 (1H, bs, NH from 3-pyrazole ring), 9.66 (1H,

575 s, NH from sec.amide), 7.38 (1H, d, J = 7.30 Hz, Ar-H), 7.28-7.14 (5H, m, Ar-H), 6.94

576 (2H, d, J = 8.7 Hz, Ar-H), 5.56 (1H, s, methine from [1, 4] thiazepin ring), 5.03 (2H, s,

577 CH$_2$), 3.68 (1H, q, J = 7.0 Hz, methine from [1, 4] thiazepin ring), 2.30 (3H, s, *ortho*

578 <u>CH$_3$</u>), 1.91 (3H, s, CH$_3$ from pyrazole ring), 1.19 (3H, d, J = 7.0 Hz, CH$_3$ from [1,4]

579 thiazepin ring); Observable minor isomer peaks are at 9.85 (1H, s, NH from

580 sec.amide), 6.99 (2H, d, J = 8.7 Hz, Ar-H), 5.32 (1H, s, methine from [1, 4] thiazepin

581 ring), 5.06 (2H, s, CH$_2$), 2.32 (3H, s, *ortho* <u>CH$_3$</u>), 1.68 (3H, s, CH$_3$ from pyrazole ring),

582 1.08 (3H, d, J = 7.2 Hz, CH$_3$ from [1, 4] thiazepin ring). HRMS- m/z (ESI): found

583 394.1586 ($C_{22}H_{24}N_3O_2S$ [M + H]$^+$), requires 394.1511.

584 *3,6-Dimethyl-4-[4-(3-methyl-benzyloxy)-phenyl]-4,8-dihydro-1H-pyrazolo[3,4-*

585 *e][1,4]thiazepin-7-one* (**1f**). Mixture of two isomers (66:34), δH/ppm (400 MHz, d^6-

586 DMSO): Major isomer peaks are at 12.31 (1H, bs, NH from 3-pyrazole ring), 9.65 (1H,

587 s, NH from sec.amide), 7.32-7.09 (6H, m, Ar-H), 6.91 (2H, d, J = 8.8 Hz, Ar-H), 5.55

588 (1H, s, methine from [1, 4] thiazepin ring), 5.01 (2H, s, CH$_2$), 3.67 (1H, q, J = 7.0 Hz,

589   methine from [1, 4] thiazepin ring), 2.31 (3H, s, *meta* <u>CH$_3$</u>), 1.90 (3H, s, CH$_3$ from

590   pyrazole ring), 1.19 (3H, d, J = 7.0 Hz, CH$_3$ from [1, 4] thiazepin ring); Observable

591   minor isomer peaks are at 9.85 (1H, s, NH from sec.amide), 7.32-7.09 (6H, m, Ar-H),

592   6.96 (2H, d, J = 8.8 Hz, Ar-H), 5.32 (1H, s, methine from [1,4] thiazepin ring), 5.03(2H,

593   s, CH$_2$), 3.24 (1H, q, J = 7.2 Hz methine from [1, 4] thiazepin ring), 2.31 (3H, s, *meta*

594 <u>CH</u>$_3$), 1.70 (3H, s, CH$_3$ from pyrazole ring), 1.01 (3H, d, J = 7.2 Hz, CH$_3$ from [1,4]

595 thiazepin ring). HRMS; m/z (ES): found 394.1580 (C$_{22}$H$_{24}$N$_3$O$_2$S [M + H]$^+$), requires

596 394.1511.

597 *3,6-Dimethyl-4-[4-(4-methyl-benzyloxy)-phenyl]-4,8-dihydro-1H-pyrazolo[3,4-*

598 *e][1,4]thiazepin-7-one* **(1g).** Mixture of two isomers (69:31), δH/ppm (400 MHz, d^6-

599 DMSO): Major isomer peaks are at 12.30 (1H, bs, NH from 3-pyrazole ring), 9.65 (1H,

600 s, NH from sec.amide), 7.36-7.27 (2H, m, Ar-H), 7.22-7.12 (4H, m, Ar-H), 6.90 (2H, d,

601 J = 8.7 Hz, Ar-H), 5.55 (1H, s, methine from [1, 4] thiazepin ring), 5.00 (2H, s, CH$_2$),

602 3.67 (1H, q, J = 7.0 Hz, methine from [1, 4] thiazepin ring), 2.29 (3H, s, *para* <u>CH</u>$_3$),

603 1.90 (3H, s, CH$_3$ from pyrazole ring), 1.18 (3H, d, J = 7.08 Hz, CH$_3$ from [1,4] thiazepin

604 ring); Observable minor isomer peaks are at 9.85 (1H, s, NH from sec.amide), 7.36-

605 7.27 (2H, m, Ar-H), 7.22-7.12 (4H, m ,Ar-H), 6.94 (2H, d, J = 8.8 Hz, Ar-H), 5.31 (1H,

606 s, methine from [1, 4] thiazepin ring), 5.01 (2H, s, CH$_2$), 3.24 (1H, q, J = 7.2 Hz

607 methine from [1, 4] thiazepin ring), 2.30 (3H, s, *para* <u>CH</u>$_3$), 1.67 (3H, s, CH$_3$ from

608 pyrazole ring), 1.07 (3H, d, J = 7.2 Hz, CH$_3$ from [1,4] thiazepin ring). HRMS; m/z (ES):

609 found 394.1582 (C$_{22}$H$_{24}$N$_3$O$_2$S [M + H]$^+$) requires 394.1511.

610 *4-(4-Benzyloxy-3-methoxy-phenyl)-3,6-dimethyl-4,8-dihydro-1H-pyrazolo[3,4-*

611 *e][1,4]thiazepin-7-one* **(1h).** Mixture of two isomers (63:37), δH/ppm (400 MHz, d^6-

612 DMSO): First isomer peaks are at 12.30 (1H, bs, NH from 3-pyrazole ring), 9.66 (1H,

613 s, NH from sec.amide), 7.50-7.27 (5H, m, Ar-H), 7.01-6.89 (2H, m, Ar-H), 6.75 (1H, dd,

614   J = 8.3 + 2.0 Hz, Ar-H), 5.51 (1H, s, methine from [1, 4] thiazepin ring), 5.02 (2H, s,

615   CH_2), 3.71 (3H, s, O$\underline{CH_3}$), 3.67 (1H, q, J = 7.0 Hz, methine from [1, 4] thiazepin ring),

616   1.95 (3H, s, CH_3 from pyrazole ring), 1.19 (3H, d, J = 7.04 Hz, CH_3 from [1,4] thiazepin

617   ring); Observable second isomer peaks are at 9.84 (1H, s, NH from sec.amide), 7.50-

618   7.27 (5H, m, Ar-H), 7.01-6.89 (2H, m ,Ar-H), 6.63 (1H, dd, J = 8.3 + 1.8 Hz, Ar-H), 5.30

619   (1H, s, methine from [1, 4] thiazepin ring), 5.04 (2H, s, CH$_2$), 3.73 (3H, s, OCH$_3$), 3.30

620   (1H, q, methine from [1, 4] thiazepin ring, this peak is partly covered by water peak

621   from DMSO), 1.68 (3H, s, CH$_3$ from pyrazole ring), 1.09 (3H, d, J = 7.2 Hz, CH$_3$ from

622   [1,4] thiazepin ring). HRMS; m/z (ES): found 410.1539 (C$_{22}$H$_{24}$N$_3$O$_3$S [M + H]$^+$)

623   requires 410.1460.

624   *4-[4-(2-Chloro-benzyloxy)-3-methoxy-phenyl]-3,6-dimethyl-4,8-dihydro-1H-*

625   *pyrazolo[3,4-e][1,4]thiazepin-7-one* **(1i).** Mixture of two isomers (72:28), δH/ppm (400

626   MHz, d^6-DMSO): Major isomer peaks are at 12.31 (1H, bs, NH from 3-pyrazole ring),

627   9.67 (1H, s, NH from sec.amide), 7.63-7.54 (1H, m, Ar-H), 7.53-7.46 (1H, m, Ar-H),

628   7.42-7.34 (2H, m, Ar-H), 7.02-6.90 (2H, m, Ar-H), 6.77 (1H, dd, J = 8.3 + 2.0 Hz, Ar-

629   H), 5.53 (1H, s, methine from [1, 4] thiazepin ring), 5.10 (2H, s, CH$_2$), 3.72 (3H, s,

630   OC$\underline{H_3}$), 3.67 (1H, q, J = 7.0 Hz, methine from [1, 4] thiazepin ring), 1.96 (3H, s, CH$_3$

631   from pyrazole ring), 1.19 (3H, d, J = 7.0 Hz, CH$_3$ from [1,4] thiazepin ring); Observable

632   minor isomer peaks are at 9.84 (1H, s, NH from sec.amide), 7.63-7.54 (1H, m, Ar-H),

633   7.53-7.46 (1H, m, Ar-H), 7.42-7.34 (2H, m, Ar-H), 7.02-6.90 (2H, m, Ar-H), 6.65 ((1H,

634   dd, J = 8.3 + 1.80 Hz, Ar-H), 5.31 (1H, s, methine from [1, 4] thiazepin ring), 5.11 (2H,

635   s, CH$_2$), 3.74 (3H, s, OC$\underline{H_3}$), 3.30 (1H, q, methine from [1, 4] thiazepin ring, this peak

636   is partly covered by water peak from DMSO), 1.69 (3H, s, CH$_3$ from pyrazole ring),

637   1.09 (3H, d, J = 7.10 Hz, CH_3 from [1,4] thiazepin ring). HRMS; m/z (ES): found

638   444.1159 ($C_{22}H_{23}ClN_3O_3S$ [M + H]$^+$) requires 444.1070.

639   *4-[4-(3-Chloro-benzyloxy)-3-methoxy-phenyl]-3,6-dimethyl-4,8-dihydro-1H-*

640   *pyrazolo[3,4-e][1,4]thiazepin-7-one* **(1j).** Mixture of two isomers (68:32), δH/ppm (400

641   MHz, d^6-DMSO): First isomer peaks are at 12.30 (1H, bs, NH from 3-pyrazole ring),

642 9.67 (1H, s, NH from sec.amide), 7.52-7.34 (4H, m, Ar-H), 7.03-6.87 (2H, m, Ar-H),

643 6.76 (1H, dd, J = 8.3 + 2.1 Hz, Ar-H), 5.52 (1H, s, methine from [1, 4] thiazepin ring),

644 5.05 (2H, s, CH$_2$), 3.72 (3H, s, OC$\underline{H}_3$), 3.67 (1H, q, J = 7.0 Hz, methine from [1,4]

645 thiazepin ring), 1.95 (3H, s, CH$_3$ from pyrazole ring), 1.20 (3H, d, J = 7.04 Hz, CH$_3$

646 from [1,4] thiazepin ring); Observable second isomer peaks are at 9.84 (1H, s, NH

647 from sec.amide), 7.52-7.34 (4H, m, Ar-H), 7.03-6.89 (2H, m ,Ar-H), 6.64 (1H, dd, J =

648 8.2 + 1.9 Hz, Ar-H), 5.30 (1H, s, methine from [1, 4] thiazepin ring), 5.10 (2H, s, CH$_2$),

649 3.74 (3H, s, OC$\underline{H}_3$), 1.68 (3H, s, CH$_3$ from pyrazole ring), 1.09 (3H, d, J = 7.2 Hz, CH$_3$

650 from [1, 4] thiazepin ring). HRMS; m/z (ES): found 444.1154 (C$_{22}$H$_{23}$ClN$_3$O$_3$S [M + H]$^+$)

651 requires 444.1070.

652 *4-[4-(4-Chloro-benzyloxy)-3-methoxy-phenyl]-3,6-dimethyl-4,8-dihydro-1H-*

653 *pyrazolo[3,4-e][1,4]thiazepin-7-one* **(1k).** Mixture of two isomers (68:32), δH/ppm (400

654 MHz, d^6-DMSO): major isomer peaks are at 12.31 (1H, bs, NH from 3-pyrazole ring),

655 9.66 (1H, s, NH from sec.amide), 7.51-7.41 (4H, m, Ar-H), 7.00-6.87 (2H, m, Ar-H),

656 6.75 (1H, dd, J = 8.4 + 2.0 Hz, Ar-H), 5.51 (1H, s, methine from [1, 4] thiazepin ring),

657 5.03 (2H, s, CH$_2$), 3.71 (3H, s, OC$\underline{H}_3$), 3.67 (1H, q, J = 7.0 Hz, methine from [1,4]

658 thiazepin ring), 1.95 (3H, s, CH$_3$ from pyrazole ring), 1.19 (3H, d, J = 7.0 Hz, CH$_3$ from

659 [1,4] thiazepin ring); Observable minor isomer peaks are at 9.84 (1H, s, NH from

660 sec.amide), 7.51-7.41 (4H, m, Ar-H), 7.00-6.87 (2H, m, Ar-H), 6.63 (1H, dd, J = 8.2 +

661 1.8 Hz, Ar-H), 5.30 (1H, s, methine from [1, 4] thiazepin ring), 5.04 (2H, s, CH_2), 3.73

662 (3H, s, O$\underline{CH_3}$), 3.30 (1H, q, methine from [1, 4] thiazepin ring, this peak is partly

663 covered by water peak from DMSO), 1.67 (3H, s, CH_3 from pyrazole ring), 1.09 (3H, d,

664 J = 7.2 Hz, CH_3 from [1,4] thiazepin ring). HRMS; m/z (ES): found 444.1157

665 ($C_{22}H_{23}ClN_3O_3S$ $[M + H]^+$) requires 444.1070.

666 *4-[3-Methoxy-4-(2-methyl-benzyloxy)-phenyl]-3,6-dimethyl-4,8-dihydro-1H-*

667 *pyrazolo[3,4-e][1,4]thiazepin-7-one* (**1l**). Mixture of two isomers (66:34), δH/ppm (400

668 MHz, d^6-DMSO): major isomer peaks are at 12.30 (1H, bs, NH from 3-pyrazole ring),

669 9.67 (1H, s, NH from sec.amide), 7.43-7.34 (1H, m, Ar-H), 7.28-7.14 (3H, m, Ar-H),

670 7.03-6.91 (2H, m, Ar-H), 6.77 (1H, dd, J = 8.3 + 2.0 Hz, Ar-H), 5.52 (1H, s, methine

671 from [1,4] thiazepin ring), 5.00 (2H, s, CH$_2$), 3.70 (3H, s, OC$\underline{H}_3$), 3.67 (1H, q, J = 7.0

672 Hz, methine from [1,4] thiazepin ring), 2.30 (3H, s, *ortho* CH$_3$), 1.96 (3H, s, CH$_3$ from

673 pyrazole ring), 1.19 (3H, d, J = 7.0 Hz, CH$_3$ from [1, 4] thiazepin ring); Observable

674 minor isomer peaks are at 9.84 (1H, s, NH from sec.amide), 7.43-7.34 (1H, m, Ar-H),

675 7.28-7.14 (3H, m, Ar-H), 7.03-6.91 (2H, m, Ar-H), 6.65 (1H, dd, J = 8.2 + 1.8 Hz, Ar-

676 H), 5.30 (1H, s, methine from [1,4] thiazepin ring), 5.02 (2H, s, CH$_2$), 3.72 (3H, s,

677 OC$\underline{H}_3$), 3.30 (1H, q, methine from [1, 4] thiazepin ring, this peak is partly covered by

678 water peak from DMSO), 2.32 (3H, s, *ortho* CH$_3$), 1.69 (3H, s, CH$_3$ from pyrazole ring),

679 1.10 (3H, d, J = 7.12 Hz, CH$_3$ from [1, 4] thiazepin ring). HRMS; m/z (ES): found

680 424.1688 (C$_{23}$H$_{26}$N$_3$O$_3$S [M + H]$^+$) requires 424.1617.

681 *4-[3-Methoxy-4-(3-methyl-benzyloxy)-phenyl]-3,6-dimethyl-4,8-dihydro-1H-*

682 *pyrazolo[3,4-e][1,4]thiazepin-7-one (1m).* Mixture of two isomers (65:35), δH/ppm (400

683 MHz, d^6-DMSO): major isomer peaks are at 12.30 (1H, bs, NH from 3-pyrazole ring),

684 9.66 (1H, s, NH from sec.amide), 7.30-7.10 (4H, m, Ar-H), 7.00-6.87 (2H, m, Ar-H),

685   6.74 (1H, dd, J = 8.3 + 2.0 Hz, Ar-H), 5.51 (1H, s, methine from [1, 4] thiazepin ring),

686   5.00 (2H, s, CH_2), 3.71 (3H, s, O$\underline{CH_3}$), 3.66 (1H, q, J = 7.07 Hz, methine from [1,4]

687   thiazepin ring), 2.31 (3H, s, *meta* CH_3), 1.95 (3H, s, CH_3 from pyrazole ring), 1.19 (3H,

688   d, J = 7.04 Hz, CH_3 from [1, 4] thiazepin ring); Observable minor isomer peaks are at

689   9.84 (1H, s, NH from sec.amide), 7.30-7.10 (4H, m, Ar-H), 7.00-6.87 (2H, m, Ar-H),

690 6.62 (1H, dd, J = 8.4 + 2.0 Hz, Ar-H), 5.30 (1H, s, methine from [1,4] thiazepin ring),

691 5.00 (2H, s, CH$_2$), 3.73 (3H, s, OC$\underline{H_3}$), 3.30 (1H, q, methine from [1,4] thiazepin ring,

692 this peak is partly covered by water peak from DMSO), 2.31 (3H, s, *meta* CH$_3$), 1.68

693 (3H, s, CH$_3$ from pyrazole ring), 1.09 (3H, d, J = 7.2 Hz, CH$_3$ from [1, 4] thiazepin ring).

694 HRMS; m/z (ES): found 424.1687 (C$_{23}$H$_{26}$N$_3$O$_3$S [M + H]$^+$) requires 424.1617.

695 *4-[3-Methoxy-4-(4-methyl-benzyloxy)-phenyl]-3,6-dimethyl-4,8-dihydro-1H-*

696 *pyrazolo[3,4-e][1,4]thiazepin-7-one (1n).* Mixture of two isomers (62:38), δH/ppm (400

697 MHz, d^6-DMSO): major isomer peaks are at 12.29 (1H, bs, NH from 3-pyrazole ring),

698 9.66 (1H, s, NH from sec.amide), 7.35-7.26 (2H, m Ar-H), 7.24-7.14 (2H, m, Ar-H),

699 7.00-6.87 (2H, m, Ar-H), 6.74 (1H, dd, J = 8.3 + 2.1 Hz, Ar-H), 5.51 (1H, s, methine

700 from [1,4] thiazepin ring), 4.97 (2H, s, CH$_2$), 3.70 (3H, s, OC$\underline{H_3}$), 3.66 (1H, q, J = 7.0

701 Hz, methine from [1,4] thiazepin ring), 2.29 (3H, s, *para* CH$_3$), 1.95 (3H, s, CH$_3$ from

702 pyrazole ring), 1.18 (3H, d, J = 7.0 Hz, CH$_3$ from [1, 4] thiazepin ring); Observable

703 minor isomer peaks are at 9.84 (1H, s, NH from sec.amide), 7.35-7.26 (2H, m Ar-H),

704 7.24-7.14 (2H, m, Ar-H), 7.00-6.87 (2H, m, Ar-H), 6.62 (1H, dd, J = 8.3 + 1.8 Hz, Ar-

705 H), 5.30 (1H, s, methine from [1,4] thiazepin ring), 4.98 (2H, s, CH$_2$), 3.72 (3H, s,

706 OC$\underline{H_3}$), 3.29 (1H, q, methine from [1, 4] thiazepin ring, this peak is partly covered by

707 water peak from DMSO), 2.30 (3H, s, *para* CH$_3$), 1.68 (3H, s, CH$_3$ from pyrazole ring),

708 709

1.09   (3H, d, J = 7.12 Hz, CH_3 from [1, 4] thiazepin ring). HRMS; m/z (ES): found 424.1687 ($C_{23}H_{26}N_3O_3S$ [M + H]$^+$) requires 424.1617.

710   *4-(4-Isopropoxy-phenyl)-3,6-dimethyl-4,8-dihydro-1H-pyrazolo[3,4-e][1,4]thiazepin-7-*

711   *one (1o).* Mixture of two isomers (97:3), δH/ppm (400 MHz, d^6-DMSO): major isomer

712   peaks are at 12.30 (1H, s, NH from 3-pyrazole ring), 9.64 (1H, s, NH from sec.amide),

713   7.15 (2H, d, J = 8.68 Hz, Ar-H), 6.80 (2H, d, J = 8.76 Hz, Ar-H), 5.54 (1H, s, methine

714 from [1, 4] thiazepin ring), 4.54 (1H, hept, <u>CH</u> of isopropyl), 3.67 (1H, q, J = 7.0 Hz,

715 methine from [1, 4] thiazepin ring), 1.90 (3H, s, CH_3 from pyrazole ring), 1.23 (6H, d, J

716 = 6.0 Hz, $(CH_3)_2$ of isopropyl), 1.18 (3H, d, J = 7.08 Hz, CH_3 from [1,4] thiazepin ring);

717 Observable minor isomer peaks are at 9.83 (1H, s, NH from sec.amide), 6.85 (2H, d, J

718 = 8.7 Hz, Ar-H), 5.30 (1H, s, methine from [1, 4] thiazepin ring), 1.67 (3H, s, CH_3 from

719 pyrazole ring), 1.07 (3H, d, J = 7.1 Hz, CH_3 from [1, 4] thiazepin ring). HRMS; m/z

720 (ES): found 332.1428 ($C_{17}H_{22}N_3O_2S$ $[M + H]^+$) requires 332.1354.

721 *3,6-Dimethyl-4-(4-propoxy-phenyl)-4,8-dihydro-1H-pyrazolo[3,4-e][1,4]thiazepin-7-one*

722 *(1p).* Mixture of two isomers (85:15), δH/ppm (400 MHz, d^6-DMSO): major isomer

723 peaks are at 12.30 (1H, s, NH from 3-pyrazole ring), 9.65 (1H, s, NH from sec.amide),

724 7.16 (2H, d, J = 8.7 Hz, Ar-H), 6.82 (2H, d, J = 8.7 Hz, Ar-H), 5.55 (1H, s, methine

725 from [1, 4] thiazepin ring), 3.87 (2H, t, J = 6.52 Hz, O<u>CH</u>₂ of n-propyl), 3.67 (1H, q, J =

726 7.0 Hz, methine from [1, 4] thiazepin ring), 1.90 (3H, s, CH_3 from pyrazole ring), 1.76-

727 1.62 (2H, m, CH_2 of n-propyl), 1.19 (3H, d, J = 7.0 Hz, CH_3 from [1,4] thiazepin ring),

728 0.95 (3H, t, J = 7.45 Hz, CH_3 of n-propyl); Observable minor isomer peaks are at 9.84

729 (1H, s, NH from sec.amide), 7.13 (2H, d, J = 8.64 Hz, Ar-H), 6.86 (2H, d, J = 8.72 Hz,

730 Ar-H), 5.30 (1H, s, methine from [1, 4] thiazepin ring), 3.90 (2H, t, J = 6.56 Hz, O<u>CH</u>₂

731 of n-propyl), 3.23 (1H, q, J = 7.17 Hz this peak is partly covered by water peak from

732 DMSO), 1.76-1.62 (2H, m, CH_2 of n-propyl), 1.06 (3H, d, J = 7.20 Hz, CH_3 from [1, 4]

733   thiazepin ring), 0.97 (3H, t, J = 7.47 Hz, CH_3 of n-propyl);   HRMS; m/z (ES): found

734   332.1428 ($C_{17}H_{22}N_3O_2S$ $[M + H]^+$) requires 332.1354.

735   *4-(4-Allyloxy-phenyl)-3,6-dimethyl-4,8-dihydro-1H-pyrazolo[3,4-e][1,4]thiazepin-7-one*

736   *(1q)*. Mixture of two isomers (97:3), δH/ppm (400 MHz, d^6-DMSO): major isomer

737   peaks are at 12.31 (1H, s, NH from 3-pyrazole ring), 9.65 (1H, s, NH from sec.amide),

738 7.17 (2H, d, J = 8.7 Hz, Ar-H), 6.85 (2H, d, J = 8.7 Hz, Ar-H), 6.09-5.94 (1H, m, =CH of

739 allyl), 5.55 (1H, s, methine from [1, 4] thiazepin ring), 5.37 [1H, dq, J = 1.71 + 17.25

740 Hz, =CH$_2$ (H$_a$-terminal vinyl proton on SP^2 carbon)], 5.23 [1H, dq, J = 1.4/1.6 + 10.5

741 Hz, =CH$_2$ (H$_b$-terminal vinyl proton on SP^2 carbon)], 4.52 [1H, t, J = 1.48, O-CH$_2$ (H$_a$-

742 allyl proton adjacent to SP^2 carbon)], 4.51 [1H, t, J = 1.48, O-CH$_2$ (H$_b$-allyl proton

743 adjacent to SP^2 carbon)], 3.67 (1H, q, J = 7.1 Hz, methine from [1, 4] thiazepin ring),

744 1.90 (3H, s, CH$_3$ from pyrazole ring), 1.19 (3H, d, J = 7.1 Hz, CH$_3$ from [1,4] thiazepin

745 ring), Observable minor isomer peaks are at 9.84 (1H, s, NH from sec.amide), 6.87

746 (2H, d, J = 8.72 Hz, Ar-H), 5.31 (1H, s, methine from [1, 4] thiazepin ring), 1.67 (3H, s,

747 CH$_3$ from pyrazole ring), 1.07 (2H, d, J = 7.1 Hz, CH$_3$ from [1, 4] thiazepin ring),

748 HRMS; m/z (ES): found 330.1272 (C$_{17}$H$_{20}$N$_3$O$_2$S [M + H]$^+$) requires 330.4180.

749 **Compounds preparation:** Benznidazole (Bz) (N-benzyl-2-nitroimidazole-1-

750 acetamide) was obtained from the Pharmaceutical Laboratory of the State of

751 Pernambuco (LAFEPE, Brazil) and used in all trials as reference drug. All the CYP51

752 inhibitor compounds were purchased from Asinex commercial vendor, diluted in

753 dimethylsulfoxide (DMSO - *in vitro*) or in trappsol (*in vivo*) not reaching vehicle levels

754 above 0.6 % and 20 % for *in vitro* and *in vivo* assays, respectively.

755 ***T. cruzi* parasites:** Bloodstream trypomastigotes (BT - *Y strain)* were obtained from

756 heart puncture of infected male Swiss Webster mice at parasitemia peak. The

757 parasites were purified and resuspended in RPMI 1640 medium (pH 7.2 to 7.4)

758   without phenol red (Gibco BRL) supplemented with 10% fetal bovine serum (FBS) and

759   2 mM glutamine, as reported previously [26, 27] The analysis upon intracellular forms

760   *T. cruzi* (Tulahuen strain transfected with *Escherichia coli* β-galactosidase gene) [28]

761 was conducted using L929 cell lineages that were infected with tissue culture-derived

762 trypomastigotes using a 10:1 parasite/ host cell ratio [27].

763 *In vitro* assays

764 **Mammalian cell culture:** The cardiac cells (CC) were obtained from Swiss embryos

765 Webster mice as described by Meirelles and coworkers [29], and seeded 96 well plate.

766 The cardiac cell cultures were stored at 37℃ in Du lbecco's modified Eagle medium

767 (DMEM; without phenol red; Sigma-Aldrich) supplemented with 5% fetal bovine serum,

768 2.5 mM CaCl$_2$, 1 mM L-glutamine, streptomycin, and 2% chicken embryo extract [22,

769 29]. Moreover, L929 fibroblastic cells were cultivated (4 x10^3 cells/well in 96-well

770 microplates) at 37℃ in RPMI 1640 medium (pH 7.2 to 7.4) without phenol red (Gibco

771 BRL) supplemented with 10% fetal bovine serum and 1% glutamine, as reported

772 previously [27, 30].

773 **Cytotoxicity assays:** To evaluate the toxicity profile and determine the selectivity

774 index (SI), cardiac and L929 cells were incubated at 37℃ with crescent

775 concentrations of the studied compounds for 24 and 96 h and cellular viability were

776 evaluated by colorimetric analysis using Prestoblue [27] and Alamarblue [30] assays

777 as reported, respectively. After 5 and 6 h of incubation respectively, the absorbance

778 were measured at 570 and 600 nm according to manufactures instructions and the

779   results confirmed by the analysis of morphology and physiology aspects through light

780   microscopy. The results are expressed as the percent of reduced viability in

781   compound-treated and vehicle-treated samples by following the manufacturer's

782   instructions and the EC_{50} values calculated (concentration that reduces the cellular

783   viability by 50%) [26, 27, 30].

784 **Trypanocidal effects:** BT forms of Y strain (5×10^6/mL) were incubated for 2 and 24 h

785 at 37℃ in absence or presence of crescent concentr ations (0 – 50 μM) of each tested

786 compound. The compounds were diluted in RPMI 1640 medium (Roswell Park

787 Memorial Institute - Sigma Aldrich – USA) supplemented with 5% FBS. Subsequently

788 the incubation, death rates were assessed by light microscopy quantification using a

789 Neubauer chamber to determine the EC_{50} that correspond the compound

790 concentration that reduces in 50% of the number of the parasite population [26,27,

791 31]. For the effect against intracellular forms (Tulahuen-β-galactosidase strain), L929

792 cells were infected for 2h, rinsed using saline to remove non-internalized parasites and

793 then incubated for 48 h at 37℃ to establish the cu lture infection. The infected L929

794 cell cultures were exposed first to a fixed concentration of tested compounds (10-12

795 μM). Those that presented ≥ 50 % of reductions in the parasite load, were further

796 screened using infected cultures submitted increasing non-toxic concentrations of the

797 selected compounds to determine the EC_{50} values.   Next, the absorbance was

798 measured at 570 nm and results expressed as the percentage of *T. cruzi* growth

799 inhibition in compound-tested cells compared to untreated cells.   In parallel, the

800 therapy using the reference drug (Bz) was always performed as reported [26].

801 *In vivo* **assay**

802   **Acute toxicity:** NOAEL (no-observed-adverse-effect level) was obtained by injecting,

803   via intraperitoneal (ip), increasing concentrations of the tested compound (up to 200

804   mg/kg of mice body weight) in female Swiss Webster mice (weight, 20 to 23 g; n - 2

805   mice per assay for two assays). Treated animals were inspected for toxic and subtoxic

806   symptoms according to the Organization for Economic Cooperation and Development

807 (OECD) guidelines. At 48 h after compound injection, the NOAEL values were

808 determined as reported previously [31].

809 **Mice infection and treatment schemes:** Male Swiss Webster mice (18 to 20 g)

810 obtained from the animal facilities of Instituto de Ciência e Tecnologia em Biomodelos

811 (ICTB) from Fundação Oswaldo Cruz (FIOCRUZ) were household at a maximum of 6

812 animals per cage, and kept in a specific-pathogen-free (SPF) room at 20 to 24℃

813 under a 12- light and 12-h dark cycle, providing sterilized water and chow *ad libitum*.

814 The animals were acclimated for 7 days before starting the experiments. Infection was

815 performed by i.p. injection of 10^4 bloodstream trypomastigotes (Y strain). Compound **1**

816 was first dissolved in DMSO and then freshly diluted with 20% of Trappsol (CTD, Inc.,

817 USA) and Bz was prepared in sterile distilled water with 3% Tween 80 (Sigma-

818 Aldrich). The animals were divided into the following groups: uninfected (noninfected

819 and untreated), untreated (infected with *T.cruzi* but treated only with vehicle), and

820 treated (infected and treated) i.p. with nontoxic doses of 5 to 20 mg/kg/day test

821 compound or with 100 mg/kg/day Bz p.o. The mouse received a 0.1-ml i.p. dose, the

822 treatment started at 5th day post infection (dpi) that represent the parasitemia onset in

823 this experimental model and followed for five consecutive days, until 9th dpi. For Bz

824 treatment, infected mice received a 0.1 mL p.o. following the same therapeutic

825 schemes as described above [19].

826 **Parasitemia and mortality rates:** Parasitemia was individually detected by Pizzy-

827 Brener [32] methodology using direct light microscopy to quantify the number of

828 parasites in 5µL of blood collected from tail vein, and the mice were checked for

829 mortality daily until 30 days post treatment [31]. Mortality was expressed by the

830 percentage of cumulative mortality (CM) as described by Batista and coworkers [22].

Ethics

All procedures were carried out in accordance with the guidelines established by the

FIOCRUZ Committee of Ethics for the Use of Animals (CEUA LW 16/14).

References

[1] World Health Organization (WHO). http://www.who.int/mediacentre/factsheets/fs340/en/, 2017 (accessed 20 November 2017).

[2] JCP. Dias, AN. Ramos Jr, ED. Gontijo, A. Luquetti, MA. Shikanai-Yasuda, JR. Coura, RM. Torres, JR. Melo, EA. Almeida, W Jr. Oliveira, AC. Silveira, JM. Rezende, FS. Pinto, AW. Ferreira, A. Rassi, AA Filho. Fragata, AS. Sousa, D. Correia, AM. Jansen, GM. Andrade, CF. Britto, AY. Pinto, A Jr. Rassi, DE. Campos, F. Abad-Franch, SE. Santos, E. Chiari, AM Hasslocher-Moreno, EF. Moreira, DS. Marques, EL. Silva, JA. Marin-Neto, LM. Galvão, SS. Xavier, AS. Valente, NB. Carvalho, AV Cardoso, RA. Silva, VM. Costa, SM. Vivaldini, SM. Oliveira, VD. Valente, MM. Lima, RV. Alves, 2 nd Brazilian Consensus on Chagas Disease, 2015. Rev da Soc Bras Med Trop. 49 (2016) 3-60.

[3] E.Chatelain, Chagas disease research and development: is there light at the end of the tunnel? Comput Struct Biotechnol J. 15 (2017) 98-103.

[4] E. Chatelain, N. Konar, Translational challenges of animal models in Chagas disease drug development: a review. Drug Des Devel Ther. 9 (2015) 4807-4823.

[5] Drugs for Neglected Diseases Initiative (DNDi). https://www.dndi.org/diseases-projects/chagas/chagas-disease-background/, 2017 (accessed 20 November 2017).

[6] MNC. Soeiro, SL. De Castro. Trypanosoma cruzi targets for new chemotherapeutic approaches. Expert Opin Ther Targets. 13 (2009)105-121.

[7] SR. Wilkinson, JM. Kelly, Trypanocidal drugs: mechanisms, resistance and new targets. Expert Rev Mol Med. 11(2009) e31.

[8] B. Zingales, MA. Miles, CB. Moraes, A. Luquetti, F. Guhl, AG. Schijman, I. Ribeiro, Drug discovery for Chagas disease should consider Trypanosoma cruzi strain diversity. Mem Inst Oswaldo Cruz. 109 (2014) 828-833.

[9] JA. Urbina, Ergosterol biosynthesis and drug development for Chagas disease. Mem. Inst. Oswaldo Cruz. 104 (2009) 311-318.

[10] MN. Soeiro, EM. de Souza, CF. da Silva, Batista Dda. G, MM. Batista, BP. Pavão, JS. Araújo, CA. Aiub, PB. da Silva, J. Lionel, C. Britto, K. Kim, G. Sulikowski, TY. Hargrove, MR. Waterman, GI, Lepesheva, *In vitro* and *in vivo* studies of the antiparasitic activity of sterol 14α-demethylase inhibitor VNI against drug-resistant strains of *T. cruzi.* Antimicrob Agents Chemother. 57(2013) 4151-4163.

[11] I. Molina, J. Gómez i Prat, F. Salvador, B. Treviño, E. Sulleiro, N. Serre D. Pou, S. Roure, J. Cabezos, L. Valerio, A. Blanco-Grau, A. Sánchez-Montalvá, X. Vidal, A. Pahissa, Randomized trial of posaconazole and benznidazole for chronic Chagas' disease. N Engl J Med. 370 (2014)1899-1908.

[12] I. Molina, F. Salvador, A. Sánchez-Montalvá, The use of posaconazole against Chagas disease. Curr Opin Infect Dis. 28 (2015) 397-407

[13] CA. Morillo, H. Waskin, S. Sosa-Estani, M. Del Carmen Bangher, C. Cuneo, R. Milesi, M. Mallagray, W. Apt, J. Beloscar, J. Gascon, I. Molina, LE. Echeverria, H. Colombo, JA. Perez-Molina, F. Wyss, B. Meeks, LR. Bonilla, P. Gao, B. Wei, M. McCarthy, S. Yusuf, Investigators. STOP-CHAGAS, Benznidazole and Posaconazole in Eliminating Parasites in Asymptomatic *T. cruzi* Carriers: The STOP-CHAGAS Trial. J Am Coll Cardiol. 69 (2017) 939-947.

[14] JA.Urbina, Pharmacodynamics and Follow-Up Period in the Treatment of Human *Trypanosoma cruzi* Infections With Posaconazole. J Am Coll Cardiol. 70 (2017) 299-300.

[15] GI. Lepesheva, Design or screening of drugs for the treatment of Chagas disease: what shows the most promise? Expert Opin Drug Discov. 8(2013)1479-1489.

[16] GI. Lepesheva, TY. Hargrove, G. Rachakonda, Z. Wawrzak, S. Pomel, S. Cojean, PN. Nde, WD. Nes, CW. Locuson, MW. Calcutt, MR. Waterman, JS. Daniels, PM. Loiseau, F. Villalta, VFV as a new effective CYP51 structure-derived drug candidate for Chagas disease and visceral leishmaniasis. J. Infect. Dis. 212 (2015) 1439-1448.

[17] WJ. Hoekstra, TY. Hargrove, Z. Wawrzak, D. da Gama Jaen Batista, CF. da Silva, AS. Nefertiti, G. Rachakonda, RJ. Schotzinger, F. Villalta, Mde N. Soeiro, GI. Lepesheva, Clinical Candidate VT-1161's Antiparasitic Effect *In Vitro,* Activity in a Murine Model of Chagas Disease, and Structural Characterization in Complex with the Target Enzyme CYP51 from *Trypanosoma cruzi.* Antimicrob Agents Chemother. 60 (2016) 1058-1066.

[18] TY. Hargrove, K. Kim, M. de Nazaré Correia Soeiro, CF. da Silva, DD. Batista, MM. Batista, EM. Yazlovitskaya, MR. Waterman, GA. Sulikowski, GI. Lepesheva, CYP51 structures and structure-based development of novel, pathogen-specific inhibitory scaffolds. Int J Parasitol Drugs Drug Resist. 2 (2012) 178-186.

[19] FH. Guedes-da-Silva, DG. Batista, CF. da Silva, MB. Meuser, MR. Simões-Silva, JS. de Araújo, CG. Ferreira, OC. Moreira, C. Britto, GI. Lepesheva, Mde N. Soeiro, Different Therapeutic Outcomes of Benznidazole and VNI Treatments in Different Genders in Mouse Experimental Models of *Trypanosoma cruzi* Infection. Antimicrob Agents Chemother. 59 (2015) 7564-7570.

[20] FH. Guedes-da-Silva, DGJ. Batista, CF. Da Silva, JS. De Araujo, BP. Pavao, MR. Simoes-Silva, MM. Batista, KC. Demarque, OC. Moreira, C. Britto, GI. Lepesheva, MNC. Soeiro, Antitrypanosomal activity of sterol 14α- demethylase (CYP51) inhibitors VNI and VFV in the Swiss mouse models of Chagas disease induced by the *Trypanosoma cruzi* Y strain. Antimicrob Agents Chemother. 61(2017) e02098-16.

[21] J. Riley, S. Brand, M. Voice, I. Caballero, D. Calvo, KD.Read, Development of a Fluorescence-based *Trypanosoma cruzi* CYP51 Inhibition Assay for Effective Compound Triaging in Drug Discovery Programmes for Chagas Disease. PLoS Negl Trop Dis. 9 (2015) e0004014.

[22] DG. Batista, MM. Batista, GM. Oliveira, PB. Amaral, J. Lannes-Vieira, CC. Brito, A.Junqueira, MM. Junqueira, AJ. Romanha, PA. Sales Junior, CE. Stephens, DW. Boykin, MN. Soeiro, Arylimidamide DB766, a potential chemotherapeutic candidate for Chagas' disease treatment. Antimicrob Agents Chemother. 54 (2010) 2940-2.

[23] SYBYL Molecular Diversity Selector, Version 7.3; Tripos, Inc.: St.Louis, MO, 2006

[24] Schrödinger Release 2017-2: Maestro, Schrödinger, LLC, New York, NY, 2017.

[25] M. De Rycker, J. Thomas, J. Riley, SJ. Brough, TJ. Miles, DW. Gray, Identification of Trypanocidal Activity for Known Clinical Compounds Using a New Trypanosoma cruzi Hit-Discovery Screening Cascade. PLoS Negl Trop Dis. 10 (2016) e0004584.

[26] BL. Timm, PB. da Silva, MM. Batista, CF. da Silva, RR. Tidwell, DA. Patrick, SK .Jones, SA. Bakunov, SM. Bakunova, Mde N. Soeiro, *In vitro* and *In vivo* Biological Effect of Novel Arylimidamide Derivatives Against *Trypanosoma cruzi*. Antimicrob Agents Chemother. 58 (2014) 3720-372.

[27] FH. Guedes-da-Silva, DGJ. Batista, MB. Meuser, KC. Demarque, TO. Fulco, JS. Araújo, PB. Da Silva, CF. Da Silva, DA. Patrick, SM. Bakunova, AS. Bakunov, RR. Tidwell, GM. Oliveira, C. Britto, OC. Moreira, MNC. Soeiro, In vitro and in vivo trypanosomicidal action of novel arylimidamides against Trypanosoma cruzi. Antimicrob Agents Chemother. 60 (2016) 2425-2434.

953 [28] FS. Buckner, CL. Verlinde, AC. La Flamme, WC, Van Voorhis, Efficient Technique
954 for Screening Drugs for Activity against *Trypanosoma cruzi* Using Parasites
955 Expressing β-Galactosidase. Antimicrob Agents Chemother. 40 (1996) 2592-2597.
956

957 [29] MNL. Meirelles, TC. Araujo-Jorge, CF. Miranda, W. de Souza, HS. Barbosa,
958 Interaction of *Trypanosoma cruzi* with heart muscle cells: ultrastructural and
959 cytochemical analysis of endocytic vacuole formation and effect upon myogenesis *in*
960 *vitro*. Eur J Cell Biol. 41(1986) 198-206.
961

962 [30] AJ. Romanha, SL. De Castro, MNC. Soeiro, J. Lannes-Vieira, I. Ribeiro, A.
963 Talvani; B. Bourdin, B. Blum, B. Olivieri, C. Zani, C. Spadafora, E. Chiari, E. Chatelain,
964 G. Chaves, JE. Calzada, JM. Bustamante, LH. Freitas-Junior, LI. Romero, MT. Bahia,
965 M. Lotrowska, M. Soares, SG. Andrade, T. Armstrong, W. Degrave, ZA. Andrade, *In*
966 *vitro* and *in vivo* experimental models for drug screening and development for Chagas
967 disease. Mem Inst Oswaldo Cruz. 105 (2010) 233-238.
968

969 [31] CF. Da Silva, DGJ. Batista, GM. Oliveira, EM. de Souza, ER. Hammer, PB. da
970 Silva, A. Daliry, JS. Araujo, C. Britto, AC. Rodrigues, Z. Liu, AA. Farahat, A. Kumar,
971 DW. Boykin, MNC. Soeiro, *In vitro* and *in vivo* investigation of the efficacy of
972 arylimidamide DB1831 and its mesylated salt form—DB1965—against *Trypanosoma*
973 *cruzi* infection. PLoS One. 7(2012) e30356.
974

975 [32] Z. Brener, Therapeutic activity and criterion of cure on mice experimentally
976 infected with *Trypanosoma cruzi*. Rev. Inst Med. trop. S. Paulo. 4 (1962) 389-396.
977
978
979
980